

AD-A049 935- AIR FORCE INST OF TECH WRIGHT-PATTERSON AFB OHIO
ON THE RAPID INTENSIFICATION OF TYPHOONS. (U)

F/6 4/2

AUG 77 C R HOLLIDAY

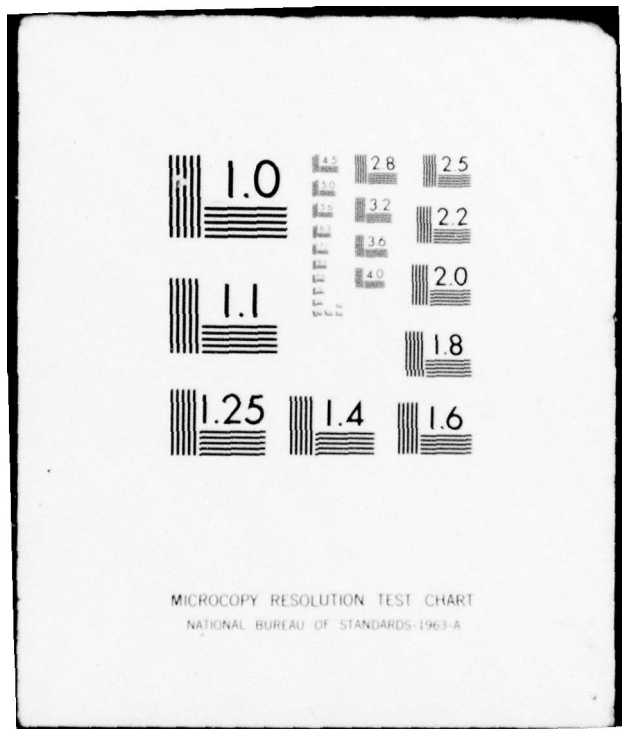
UNCLASSIFIED

AFIT-CI-78-27

NL

1 OF 2
AD
A049935





AD A 049935

AD No.
DRAFT FILE COPY

ON THE RAPID INTENSIFICATION OF TYPHOONS

78-27

1

A Thesis

by

CHARLES RICHARD HOLLIDAY

Submitted to the Graduate College of
Texas A&M University
in partial fulfillment of the requirement for the degree of

MASTER OF SCIENCE

August 1977

Major Subject: Meteorology

D D C
RECEIVED
FEB 14 1978
RECORDED

DISTRIBUTION STATEMENT A
Approved for public release;
Distribution Unlimited

UNCLASSIFIED

SECURITY CLASSIFICATION OF THIS PAGE (When Data Entered)

REPORT DOCUMENTATION PAGE			READ INSTRUCTIONS BEFORE COMPLETING FORM
1. REPORT NUMBER 14 AFIT-CI-78-27	2. GOVT ACCESSION NO.	3. RECIPIENT'S CATALOG NUMBER	
4. TITLE (and subtitle) On the Rapid Intensification of Typhoons		5. TYPE OF REPORT & PERIOD COVERED 9 Master's Thesis	
6. AUTHOR(s) 10 Captain Charles R. Holliday		7. PERFORMING ORG. REPORT NUMBER	
8. CONTRACT OR GRANT NUMBER(s)		9. PERFORMING ORGANIZATION NAME AND ADDRESS AFIT/CI Student at Texas A&M University, College Station, Texas	
10. PROGRAM ELEMENT, PROJECT, TASK AREA & WORK UNIT NUMBERS		11. CONTROLLING OFFICE NAME AND ADDRESS AFIT/CI WPAFB OH 45433	
12. REPORT DATE 11 Aug 1977		13. NUMBER OF PAGES 88 Pages 101p.	
14. MONITORING AGENCY NAME & ADDRESS (if different from Controlling Office)		15. SECURITY CLASS. (of this report) Unclassified	
16. DISTRIBUTION STATEMENT (of this Report) Approved for Public Release; Distribution Unlimited		15a. DECLASSIFICATION/DOWNGRADING SCHEDULE	
17. DISTRIBUTION STATEMENT (of the abstract entered in Block 20, if different from Report)			
18. SUPPLEMENTARY NOTES for James E. Skarath JERAL F. GUESS, Captain, USAF Director of Information, AFIT		APPROVED FOR PUBLIC RELEASE AFR 190-17. MSGt, USAF Deputy Director of Information	
19. KEY WORDS (Continue on reverse side if necessary and identify by block number)			
20. ABSTRACT (Continue on reverse side if necessary and identify by block number)			
012 200			

ACCESSION for	
STL	White Section <input checked="" type="checkbox"/>
BLW	Buff Section <input type="checkbox"/>
UNARMED	
JUSTIFICATION	
BY	
DISTRIBUTION/AVAILABILITY CODES	
DISL	AVAIL. and/or SPECIAL
A	

ON THE RAPID INTENSIFICATION OF TYPHOONS

A Thesis

by

CHARLES RICHARD HOLLIDAY

Approved as to style and content by:

Aylmer H. Thompson

(Chairman of Committee)

Vance Mozer
for (Head of Department)

Phanindramohan Das

(Member)

Dwian Djuric
(Member)

Wink Steinert
(Member)

August 1977

D D C
RECORDED
FEB 14 1978
RECORDED
D

DISTRIBUTION STATEMENT A
Approved for public release; Distribution Unlimited

ABSTRACT

On the Rapid Intensification of Typhoons (August 1977)

Charles Richard Holliday, B.A., University of Maryland

Chairman of Advisory Committee: Dr. A. H. Thompson

The occurrence of rapid deepening of tropical cyclones (≥ 42 mb, in 24 h) in the western North Pacific is examined to determine the statistics of these events, and identify features peculiar to their onset. Seventy-nine cases of rapid growth during the period 1956-1976 were selected to study climatological characteristics. These data show that the majority (75%) of the deep central pressures (≤ 920 mb) in the region are attained through the rapid growth process. The bulk (67%) of these pressure reductions occur over a short time interval of 18 h or less with the first 6 h most likely to account for the steepest fall.

The statistics reveal that development of a tropical cyclone to typhoon intensity over warm waters (temperature $\geq 28^{\circ}\text{C}$ to a depth of 30 m) is a necessary (but not sufficient) prerequisite for rapid deepening. An eye dimension near 20 n mi also is a frequently observed feature at the onset of rapid deepening. The time of onset occurs most frequently at night. Investigation of typhoon track direction and speed (or changes of these two variables) in relation to abrupt intensification revealed little association.

Ten storms displaying explosive intensification (≥ 60 mb in 24 h) and an equal number of slow to normal-developing storms (≤ 24 mb in 24 h) were compared to identify contrasts in the patterns of

upper tropospheric (200 mb) circulation influences. The main difference found was the accessibility of multiple outflow channels from the tropical cyclone. The area of outflow (5-10° from the center) characteristic of the more rapidly developing storms was observed to have an azimuthal spread twice as large as the slowly growing storms. Also, the rapidly growing typhoons exhibited a total outflow magnitude three times that of the slower developing storms.

ACKNOWLEDGEMENTS

The author's graduate program was sponsored and financed by the Air Force Institute of Technology, U. S. Air Force.

In addition, I wish to express appreciation to:

Dr. A. H. Thompson, my committee chairman, for providing excellent office facilities, and valuable assistance during the final preparation of this thesis.

Dr. D. Djuric, committee member, for his practical and timely advice, and encouragement throughout this investigation.

Dr. P. M. Das, Dr. R. K. Steinhorst, committee members, and Dr. V. E. Moyer, for their aid in reviewing the final manuscript.

Professor J. C. Sadler of the University of Hawaii, and the Joint Typhoon Warning Center, Guam for providing the necessary data.

Cindy Brooks, and Leslie Lea for their typing and drafting support.

My wife, Suzan, whose patience and understanding were essential to the completion of my program.

TABLE OF CONTENTS

	Page
ABSTRACT.	iii
ACKNOWLEDGEMENTS.	v
TABLE OF CONTENTS	vi
LIST OF FIGURES	viii
LIST OF TABLES.	xii
1. INTRODUCTION	1
2. BACKGROUND	2
3. DEEPENING STAGE.	6
a. Data discussion.	6
b. Procedure.	7
c. Criterion for rapid deepening.	8
d. Development types.	8
e. Minimum pressures attained	12
f. Duration and rates of development.	13
g. Relation of onset of intensification to time of day.	17
4. ASPECTS OF STORM ORGANIZATION.	20
a. Formation period	20
b. Intensity at onset of rapid deepening.	25
c. Size of eye-cloud wall system.	28
5. TRAJECTORY AND SEASONAL--GEOGRAPHIC ASPECTS.	33
a. Trajectory direction and speed	33

TABLE OF CONTENTS (continued)

	Page
b. Seasonal distribution.	38
c. Geographic distribution.	40
1) Ocean temperature influences.	45
2) Upper tropospheric influences	55
6. OUTFLOW CHARACTERISTICS.	61
a. Introduction	61
b. Data discussion.	62
c. Results.	66
7. SUMMARY.	76
8. RECOMMENDATIONS.	79
REFERENCES.	81
APPENDIX.	85
VITA.	88

LIST OF FIGURES

Figure	Page
1. Frequency distribution of maximum 24-h deepening of typhoons (1956-1976)	10
2. Cumulative frequency distribution of maximum 24-h deepening of typhoons (1956-1976)	10
3. History of central pressure readings for typhoons typical of type 1 development (Kit, June 1966; and Fran, September 1976). Arrow indicates onset of rapid deepening ($\geq 1.75 \text{ mb h}^{-1}$)	11
4. History of central pressure readings for typhoons typical of type 2 development (Virginia, June 1957; and Anita, August 1970). Arrow indicates onset of rapid deepening ($\geq 1.75 \text{ mb h}^{-1}$)	11
5. Relation between minimum central pressure of deep typhoons ($< 920 \text{ mb}$) and the maximum 24-h pressure fall	14
6a. Central pressure fall rates within given time periods for rapidly deepening typhoons. (Isopleths are of equal numbers of occurrences.)	15
6b. Same as Fig. 6a except isopleths are percentage of minimum criterion for rapid deepening (42 mb in less than 24 h)	16
7. Period when maximum central pressure fall occurred during rapid deepening	16
8. Time elapsed from origin (weak circulation stage) to onset of rapid deepening	21
9. Origin points (weak circulation stage) of rapid developing typhoons	22
10. Time elapsed from tropical storm generation to onset of rapid deepening	24

LIST OF FIGURES (continued)

Figure	Page
11. Frequency distribution of central sea-level pressure at onset of rapid deepening.	25
12a. Frequency distribution of time elapsing between initiation of rapid deepening and typhoon generation.	27
12b. Cumulative frequency distribution of time elapsing between initiation of rapid deepening and typhoon generation.	27
13. Frequency distribution of eye diameter at onset of rapid deepening, and 12 and 24 h after that time	30
14. Mean 24-h direction of typhoon track immediately prior to rapid deepening vs. mean 24-h direction during rapid deepening period	34
15. Mean 24-h typhoon speed immediately prior to rapid deepening vs. 24-h speed during the rapid deepening period.	36
16. Annual distribution of rapidly deepening typhoons (1956-1976)	39
17. Distribution of rapid deepening during main activity period (by $\frac{1}{2}$ month periods).	39
18. Typhoon track segments (1956-1976) for period of rapid deepening (24 h) during summer and early fall (20 June-16 October)	41
19. Typhoon track segments (1956-1976) for period of rapid deepening (24 h) during late fall through spring (November-May)	42
20. Areas where typhoons intensified rapidly during summer and early fall (20 June-16 October) --number of occurrences (1956-1976)	43
21. Areas where typhoons intensified rapidly during late fall through spring (November-May) --number of occurrences (1956-1976)	44

LIST OF FIGURES (continued)

Figure	Page
22. July mean positions of the 28°C ocean temperature isotherm (sfc., 30,-and 60-m depth), and the 200-mb Tropical Upper Tropospheric Trough (TUTT). Typhoon track segments denoting period of rapid deepening for both June (last week) and July are indicated.	49
23. August mean position of the 28°C ocean temperature isotherm (sfc., 30,-and 60-m depth), and the 200-mb Tropical Upper Tropospheric Trough (TUTT). Typhoon track segments denoting period of rapid deepening for August are indicated	50
24. September mean position of the 28°C ocean temperature isotherm (sfc., 30,-and 60-m depth), and the 200-mb Tropical Upper Tropospheric Trough (TUTT). Typhoon track segments denoting period of rapid deepening for September are indicated.	51
25. October mean position of the 28°C ocean temperature isotherm (sfc., 30,-and 60-m depth), the mean position of the 200-mb Subtropical Ridge (STR), and the average position (between September and October) of the Tropical Upper Tropospheric Trough (TUTT). Typhoon track segments denoting period of rapid deepening for October (all within first 16 d) are indicated	52
26. November mean position of the 28°C ocean temperature isotherm (sfc., 30,-and 60-m depth), and the 200-mb Subtropical Ridge (STR). Typhoon track segments denoting period of rapid deepening for November are indicated.	53
27. December mean position of the 28°C ocean temperature isotherm (sfc., 30,-and 60-m depth), and the 200-mb Subtropical Ridge (STR). Typhoon track segments denoting period of rapid deepening for December and the first week of January are indicated	54

LIST OF FIGURES (continued)

Figure	Page
28. Schematic of storm outflow interaction (dashed lines) with the larger scale circulation (solid lines). STR is the Subtropical Ridge; SER, the Subequatorial Ridge; and TUTT, the Tropical Upper Tropospheric Trough. (From Sadler, 1976a)	56
29. ITOS-1 satellite view of typhoon Betty (12 August 1972) with cloudiness features south of the typhoon depicting outflow into the upper tropospheric easterlies.	58
30. ITOS-1 satellite view of typhoon Anita (20 August 1970) with cloudiness absent equatorward of the typhoon indicating outflow to the upper tropospheric easterlies has been severed.	59
31. Upper tropospheric data typically available for analysis, including conventional rawinds, transient aircraft Doppler measurements, and flow direction derived from cirrus clouds depicted in satellite imagery. (Typhoon Hope, 0000 GMT 23 September 1970)	65
32. Composite 200-mb radial wind component field for ten extreme deepening typhoons (≥ 60 mb in 24 h)	67
33. Composite 200-mb radial wind component field for ten slow to normal deepening typhoons (≤ 24 mb in 24 h)	68
34. ITOS-1 satellite view of typhoon Hope (23 September 1970) that depicts typhoon outflow interaction with upper tropospheric cold low 700 n mi to the northwest (c)	71
35. Radial wind component field ($m s^{-1}$) for upper tropospheric level (150 mb), Hurricane Celia, 1600 GMT 3 August 1970.	75

LIST OF TABLES

Table	Page
1. Cases used to determine maximum 24-h deepening.	9
2. Time of occurrence of onset of rapid deepening.	18
3a. Frequency distribution of eye diameters for western North Pacific tropical cyclones developing to typhoon force.	31
3b. Same as table 3a but stratified for central pressure	31
4. Sea-surface temperature variation associated with rapid deepening (1959-1976)--62 cases	46
5. Subsurface climatological temperature variation associated with rapid deepening (1959-1976)--62 cases	48
6. Typhoons selected for analysis	63
7. Preferred outflow sectors, 5-10° from Center, (outward radial component \geq 7 kt for each data point)	
a. Extreme deepening (\geq 60 mb per day)	
b. Slow or normal deepening (\leq 24 mb per day)	69
8. Total flow, 5-10° from Center, and size of typhoon	73

1. INTRODUCTION

Intensity prediction is recognized as one of the more difficult typhoon¹ forecasting problems. Development may occur with almost explosive suddenness, in a period of less than a day, or hesitatingly over several days. The development of skill for recognizing the vigorous deepening circumstance is of particular importance due to the possible serious consequences to islands, coastal mainland, and shipping in close proximity. However, abrupt intensification has received relatively little attention in research to date. Efforts described in this paper are directed toward obtaining statistics on these events for the western North Pacific area, and establishing some antecedent criteria for identifying this type of development.

¹The terms "hurricane" and "typhoon" are regional and indicate a class of tropical cyclone in which maximum winds in the circulation are ≥ 64 kt (32 m sec^{-1})

The citations in this paper follow the style of the Journal of Applied Meteorology.

2. BACKGROUND

Current prediction techniques for intensity of tropical cyclones are composed largely of extrapolation of trends, use of climatology, employment of analog techniques or combinations of these methods. Brand and Gaya (1971) compiled a climatology (1945-1969) of observed intensity changes (maximum winds) for 12, 24, and 48 h for 10° squares of the western North Pacific stratified by month and stage of development. Two statistical analogue prediction techniques (that utilize regression equations for 24, 48, 72 h and a historical tape file) have been produced for the western North Pacific. One technique forecasts the central pressure (Wagoner, 1973), and the other estimates maximum winds (Elsberry et al., 1974). Dvorak (1975) has developed a scheme which combines analysis of satellite imagery with a model of tropical cyclone intensification. This method utilizes a combination of past trend with a climatological development curve and an interpretation of general cloudiness features (based on visual satellite imagery, once a day) to predict intensity after 24 h.

Although these objective techniques show ability to forecast intensity changes in the normal situation, experience has shown shortcomings in these methods for abnormally rapid intensification or decay. The development of skill for recognizing these abnormal situations is thus of importance. However, the specific case of rapid development has received relatively little emphasis in the literature.

Two studies have focused on some climatological characteristics

of the vigorously deepening typhoon. Ito (1963) performed a study of typhoon development (1950-1961) and identified the Philippine Sea south of 25° N as the geographic region with greatest frequency of rapid deepening ($\geq 2.0 \text{ mb h}^{-1}$). Later Brand (1973) examined accelerated development in terms of rate of change in maximum winds ($\geq 10 \text{ mb h}^{-1}$) 1945-1969. His results showed distinct geographic and seasonal preferences for this phenomenon.

Most explanations for changes in intensity of tropical cyclones relate to the outflow mechanism at high levels first pointed out by Riehl (1954). He emphasized the need for high-level cold advection on the storm's periphery to remove the excess heat. Riehl (1956) and Miller (1958) examined the 200-mb patterns favorable for intensification of a few hurricanes during 1954-1955. Although some characteristic patterns were noted, lack of sufficient data at upper levels over the oceans hindered investigations.

Colon and Nightingale (1963) investigated a larger number of cases. They considered favorable flow above tropical cyclones of various stages of development (depression to minimal strength). In examining cases in the Atlantic, they concluded that poleward flow aloft (such as found on the eastern side of troughs in the westerlies, tropical upper cold lows, or on the western side of anticyclones) was more conducive for development than equatorward flow. As with other investigations, lack of data over the ocean areas hampered their analysis.

The availability of routine daily satellite coverage by the late 1960's helped fill some of the data voids. A study by Shenk and

Rodgers (1974) of several periods within the life cycle of hurricane Camille (August 1969) utilized satellite imagery. Just prior to significant deepening, infrared data showed that a pronounced band of cloudiness had formed southeastward from the center. This was reasoned to be associated with the rapid transport of moisture into the storm circulation.

Later an examination of the rapid intensification of hurricane Celia (August 1970) by Clark (1975) made no mention of such a band. However, he suggested that significant development was, in part, caused by a major change in the direction of surface inflow over warm shelf waters of shallow depth. Ramage (1974) investigated the intensity changes of three South China Sea typhoons (October 1970). He found, however, that ocean temperature distribution did not control typhoon intensity but development responded to influences of troughs in the upper tropospheric subtropical westerlies.

Recently, Sadler (1976a, 1976b) stressed the importance of multi-directional outflow channels for controlling the intensity changes in typhoons. His studies of the western North Pacific (July 1972, August 1973) have shown that during the summer the storm's interaction with the Pacific Tropical Upper Tropospheric Trough, as well as its outflow to the equatorial easterlies, plays an important role in a typhoon's ultimate intensity and the associated development rate.

This study was initiated as an attempt to further document the climatological characteristics of rapidly developing typhoons, and by examination of several individual cases of extreme intensification,

to gain some observational insight into favorable upper tropospheric circulation patterns.

3. DEEPENING STAGE

a. Data discussion

Rapid intensification is best evaluated by the rate of fall of the central pressure of the typhoon. Central pressure is considered a more reliable and conservative measure of intensity than the maximum winds,² and is not as likely to be biased by sampling procedures of aircraft reconnaissance (Colon, 1963; Sheets and Grieman, 1975).

Readings of central pressure obtained by aircraft reconnaissance in the western North Pacific area were extracted from copies of the Annual Typhoon Report published by the Joint Typhoon Warning Center (JTWC), Guam. Since the majority of typhoon penetrations was conducted at the 700-mb level, a regression equation developed by Jordan (1958) to determine central sea level pressure based on the minimum 700-mb geopotential height was used to check the consistency of the eye dropsonde readings. The main purpose here was to screen for copy errors and raw surface pressure readings which had not been computed by use of thickness values. Maximum measurement errors for the dropsonde are considered to be ± 6 mb (Meyer, 1971). For any data falling outside these limits, the sea-level pressure determined by the regression equation was used. The period 1956-1976 was thus selected for study due to the availability of 700-mb geopotential height data in these annual reports. A 24-h interval was chosen for examination of maximum deepening as reconnaissance observations were

²Large variations in actual wind speeds are often noted to occur on relatively small scales in time and space (Sheets, 1972).

available at least once a day during the earlier years, and this interval coincides conveniently with a standard forecast period.

b. Procedure

Plots of the history of central pressure were prepared for each typhoon during the period of study. Maximum 24-h deepening during each lifetime was then tabulated. Sufficient pressure data were not available for 53 typhoons to determine maximum 24-h deepening. In most cases, these were storms in which the first reconnaissance revealed an already well-developed typhoon, and further intensification was slight. Also many developing storms near mainland China in the South China Sea were only incompletely reconnoitered due to aircraft restrictions. In addition, several typhoons listed in the annual reports through 1966 failed to meet minimum requirements for typhoon-strength winds based on the central pressure-maximum wind relationship developed by Atkinson and Holliday (1977). The inclusion of such storms as typhoons, no doubt, was influenced by subjective estimates of maximum winds based on the state of the sea. The question of accuracy of these estimates has been discussed by Jordan and Fortner (1960, 1961). The value of 985 mb for the central pressure was used as a screen since it was located at the upper limit of one standard error of estimate for typhoon intensity. This restriction eliminated an additional 27 cases. Thus, from the total of 385 typhoons counted during the 21-yr period, 80 cases had to be discarded. A breakdown of the remaining cases by year is presented in

Table 1. These 305 typhoons are considered to constitute a reasonable sample upon which to build reliable statistical conclusions.

c. Criterion for rapid deepening

A frequency distribution of maximum 24-h deepening for the useable data is shown in the form of a histogram in Fig. 1 and arranged into class intervals of 10 mb. The data show a distribution skewed toward the smaller deepening rates with maximum frequencies (53% of the sample) occurring in the 10-29 mb d^{-1} interval. The observations ranged from 5 mb to 95 mb d^{-1} with a mean of 29.7 mb d^{-1} and a standard deviation of 18.6 mb d^{-1} . Fig. 2 shows a cumulative frequency of the data with the median centered at 24 mb d^{-1} . It was felt appropriate to designate those cases in the upper 25% of the sample as rapid-growth systems. This portion of the sample was increased slightly (0.6%) to provide a convenient cut-off in the hourly deepening rate for classification purposes. Thus a rate of ≥ 1.75 mb h^{-1} for 24 h or ≥ 42 mb d^{-1} was chosen to identify rapid intensification. A list of the 79 typhoons comprising this sample appears in the Appendix.

d. Development types

Two basic categories of pressure profiles were noted when examining rapidly intensifying storms. Fig. 3 shows a typical example of the first group (type 1). The central pressure falls at a moderate rate (≥ 0.8 mb h^{-1}) at least for 12-24 h, followed abruptly by accelerated development (≥ 1.75 mb h^{-1}). Thirty-six percent of the

Table 1. Cases used to determine maximum 24-h deepening.

Year	1 Typhoon Count in ATR [†]	2 Incomplete Data	3 Below Typhoon Intensity*	4 Total Used
1976	15	4	0	11
1975	13	1	0	12
1974	15	0	0	15
1973	11	2	0	11
1972	22	4	0	16
1971	24	1	0	23
1970	12	0	0	12
1969	13	3	0	10
1968	20	0	0	20
1967	20	2	0	18
1966	19	1	3	25
1965	21	2	5	14
1964	26	1	5	20
1963	19	3	1	15
1962	23	3	2	18
1961	20	9	1	10
1960	19	4	2	13
1959	17	1	1	15
1958	20	5	3	12
1957	18	5	0	13
1956	18	2	4	12
Total	385	53	27	305
% of Column 1		14%	7%	79%

† ATR - Annual Typhoon Report

* Based on central pressure-maximum wind relationships.

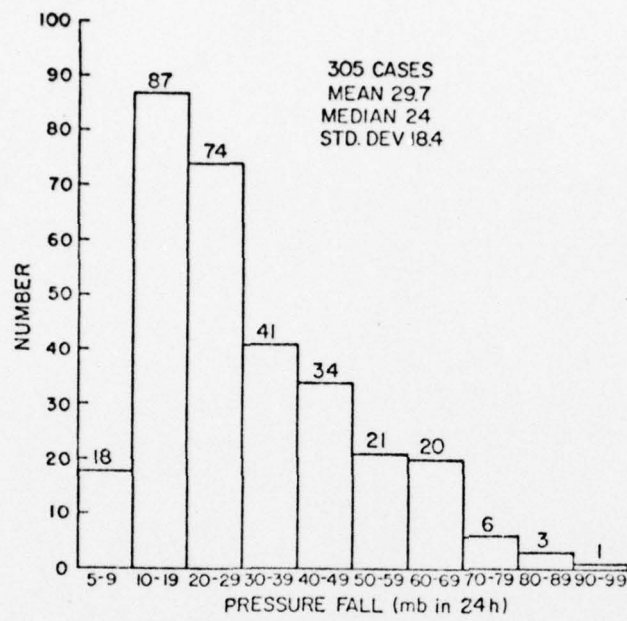


Fig. 1. Frequency distribution of maximum 24-h deepening of typhoons (1956-1976).

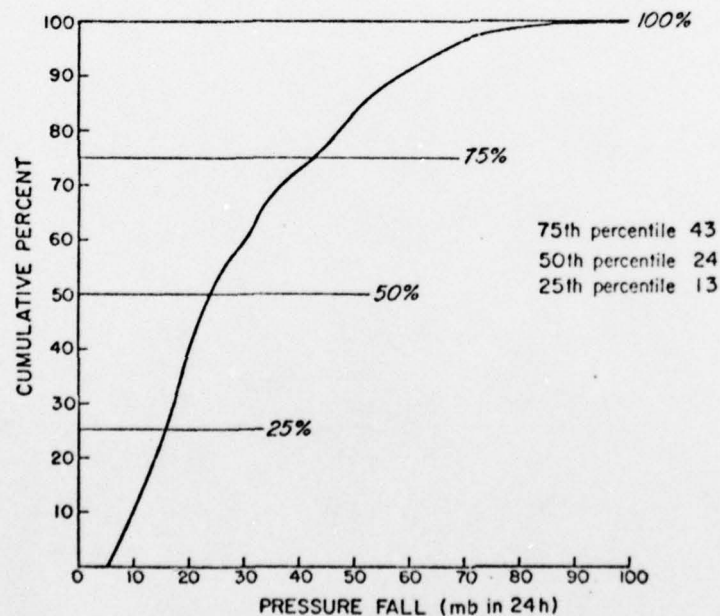


Fig. 2. Cumulative frequency distribution of maximum 24-h deepening of typhoons (1956-1976).

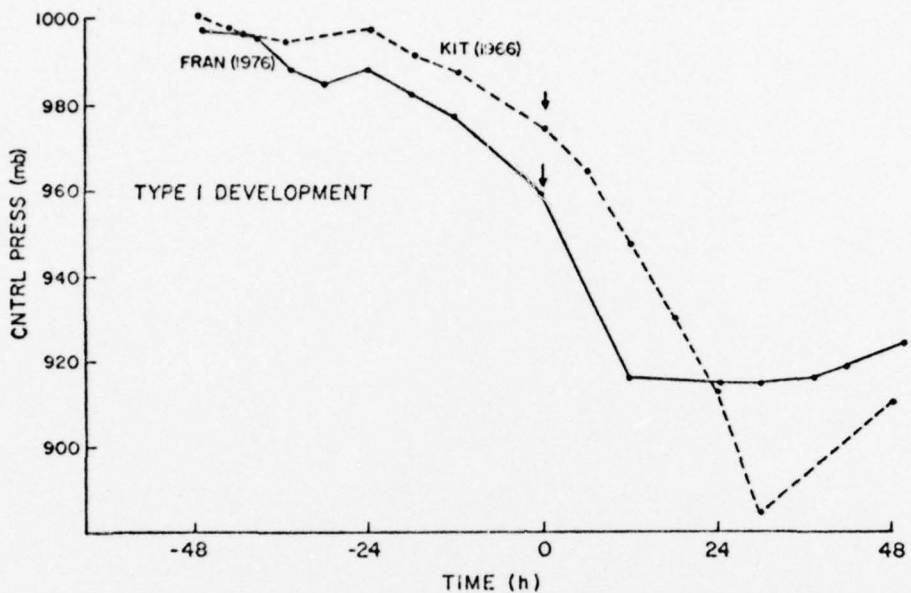


Fig. 3. History of central pressure readings for typhoons typical of type 1 development (Kit, June 1966; and Fran, September 1976). Arrow indicates onset of rapid deepening ($\geq 1.75 \text{ mb h}^{-1}$).

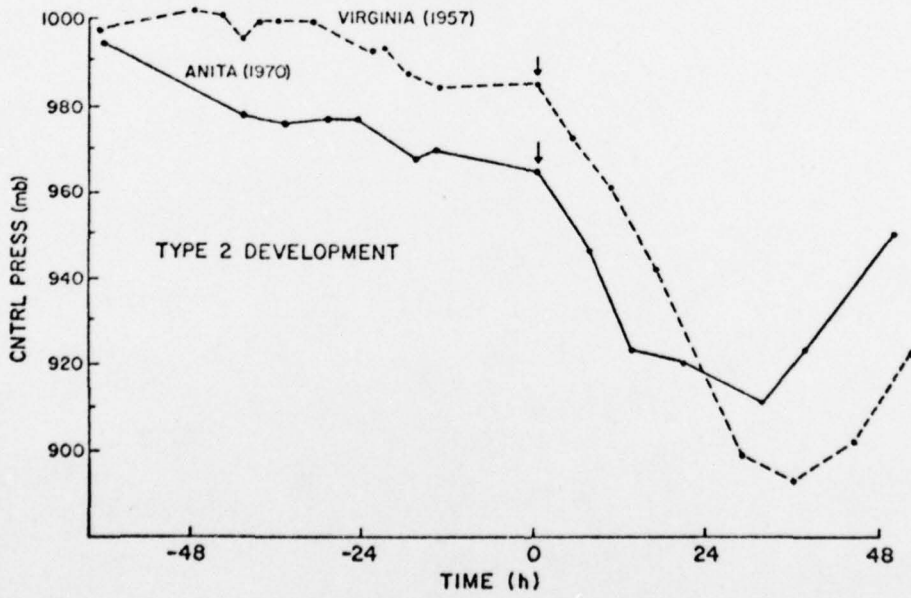


Fig. 4. History of central pressure readings for typhoons typical of type 2 development (Virginia, June 1957; and Anita, August 1970). Arrow indicates onset of rapid deepening ($\geq 1.75 \text{ mb h}^{-1}$).

sample displayed this type of behavior. Changes in the central pressure for the cases plotted (Typhoon Kit 1966, and Fran 1976) show a fall rate near 1 mb h^{-1} for 24 h prior to the onset of the most rapid development (marked by arrow). Kit's vigorous deepening lasted for 30 h at a rate of 2.6 mb h^{-1} while Fran's increased intensification lasted 12 h at a rate of 3.6 mb h^{-1} .

Type 2 behavior is characterized by slower initial development ($<0.8 \text{ mb h}^{-1}$) suddenly followed by a surge of deepening ($\geq 1.75 \text{ mb h}^{-1}$). The eye central pressure readings for Typhoons Virginia (1957) and Anita (1970) plotted in Fig. 4 are representative of such development. Circulation growth is slow at first, with 8 and 12 mb drops in 24 h for Virginia and Anita (0.3, and 0.5 mb h^{-1} respectively). These are followed by an abrupt reduction in central pressure (marked by arrow). In the case of Virginia, the pressure plummeted 86 mb in 30 h (2.9 mb h^{-1}) while the fall duration for Anita was shorter (12 h), measuring 36 mb (3.8 mb h^{-1}). This type of development was dominant in the sample and accounted for 64% of the cases.

e. Minimum pressures attained

In reviewing the cases of rapid growth it was interesting to note that a majority (75%) resulted in very deep central pressures ($\leq 920 \text{ mb}$). This classification has been used by Fung (1970), and earlier by Frank and Jordan (1960), to identify extreme typhoons. A total of 71 of all the typhoons occurring during the period 1956-1976 reached intensities severe enough to be placed in this category. In order to determine the prevalence of such minimum pressure following a rapid

drop of central pressure, a scatter diagram was constructed to compare these minima against the maximum 24-h fall rate. The diagram (Fig. 5) indicates a strong preference for these deep pressures to occur following a vigorous deepening. (In fact, record extremes occurring below 885 mb were all obtained in this manner.) Only 14% of the 71 cases displayed a more gradual rate of development (<42 mb per day).

f. Duration and rates of development

The central pressure history for each typhoon was examined to determine maximum rates of fall over various time periods during the duration of rapid intensification (6, 12, 18 h as well as 24 h with some cases extending to 30, and 36 h). The numbers of occurrences for each fall rate (mb h^{-1}) over these individual time intervals are shown in Figs. 6a and 6b. As consecutive 6 h observations were not always available for each typhoon, the complete sample is not represented for all times (number of cases are noted at bottom of each column). Isopleths of number of occurrences are shown in Fig. 6a, while the isolines in Fig. 6b indicate ratios of the actual rate of deepening to the minimum criterion for rapid deepening (42 mb in 24 h or less). In the case of Fig. 6b data points right of the 75% isopleth, but left of 100% isopleth indicate falls of greater than 31 but less than 42 mb (for example, 3.0 mb h^{-1} for 12 h is 36 mb).

The general picture portrayed by the diagrams is that rapidly developing typhoons sustain the bulk of their pressure fall over short time scales, and durations of fall rates of 1.75 mb h^{-1} beyond 24 h

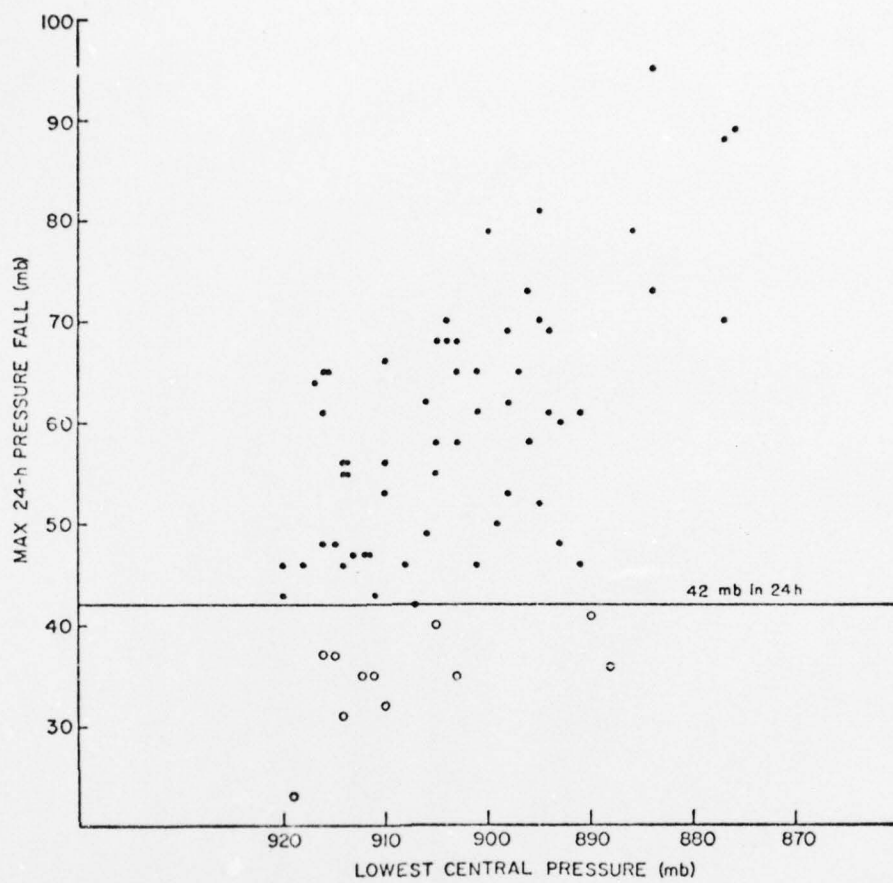


Fig. 5. Relation between minimum central pressure of deep typhoons (≤ 920 mb) and the maximum 24-h pressure fall.

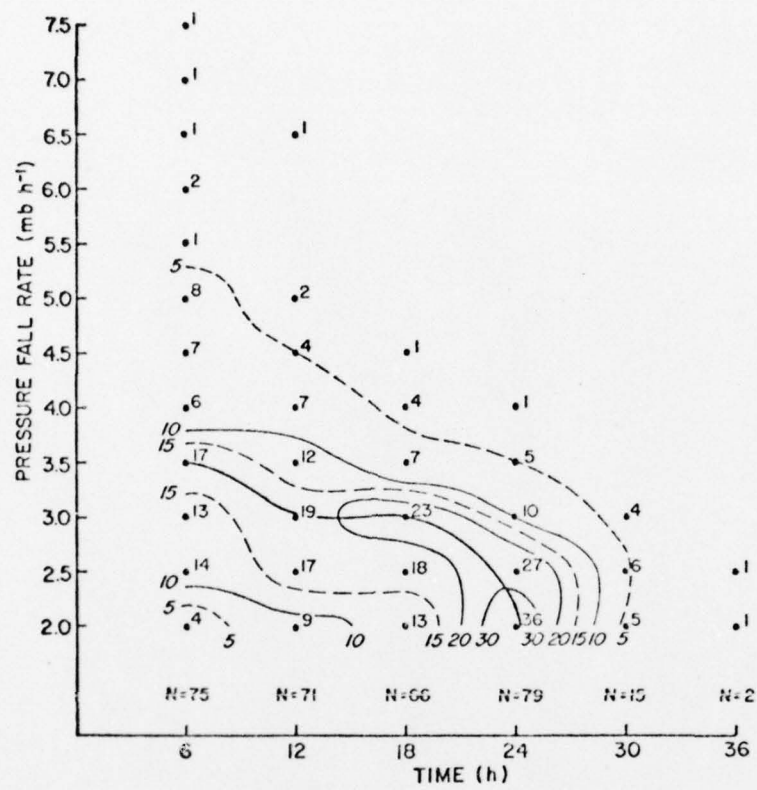


Fig. 6a. Central pressure fall rates within given time periods for rapidly deepening typhoons. (Isopleths are of equal numbers of occurrences.)

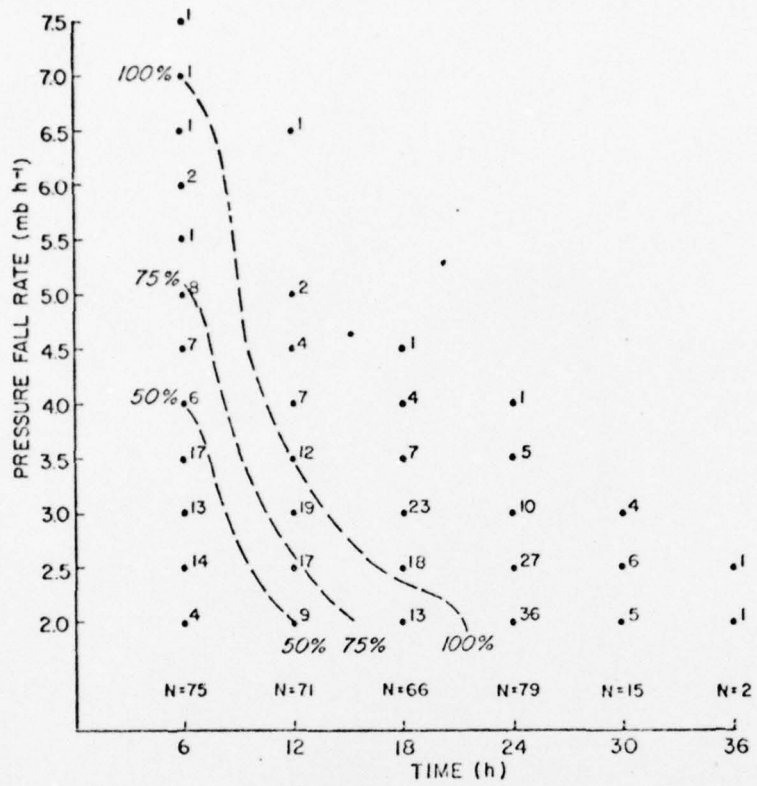


Fig. 6b. Same as Fig. 6a except isopleths are percentage of minimum criterion for rapid deepening (42 mb in less than 24 h).

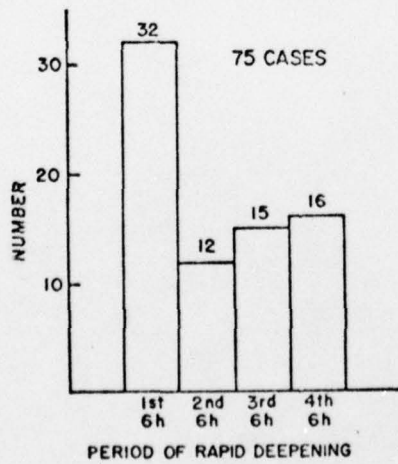


Fig. 7. Period when maximum central pressure fall occurred during rapid deepening.

are relatively uncommon. Examples of some of the more extreme cases include Opal 1967 (44 mb in 6 h), Irma 1971 (41 mb in 6 h) and Vera 1959 (39 mb in 6 h). The relative frequencies indicate that 20 mb is a fairly common fall in 6 h and is slightly less (46%) than half the minimum criterion for rapid deepening (42 mb) within a day. Data presented in Fig. 7 show these peak falls are most likely to occur during the first 6 h of the period. Extremes for half a day include Irma 1971 (77 mb in 12 h) and Vera 1959 (58 mb in 12 h). It is noted here that the majority (44) of the incidences recorded have deepened at least 75% of the 24-h criterion for rapid growth. By 18 h the bulk of occurrences (53) have reached 100%. Maxima for this period consist of Irma 1971 (85 mb in 18 h), June 1975 (77 mb in 18 h) and Ida 1958 (77 mb in 18 h). Peaks for 24-h deepening included the same typhoons with rates of 95, 89 and 88 mb, respectively.

It is noteworthy that the duration of rapid deepening extended to 30 h in some cases (15 typhoons). Some of the more striking individual examples were Kit 1966 (89 mb in 30 h) and Ida 1958 (95 mb in 30 h). Both Louise 1976 (58 mb in 36 h) and Elaine 1968 (83 mb in 36 h) accounted for those typhoons of longest duration with fall rates $\geq 1.75 \text{ mb h}^{-1}$.

g. Relation of onset of intensification to time of day

Over the years observers aboard both operational and research aircraft missions have remarked that hurricanes appear more active at night than during the day (Sheets, 1969). A study by Sheets (1972) of maximum wind changes in hurricanes (1961-1968), however, indicates

no significant diurnal variation of hurricane intensity. To determine if any preferred time of day might be prevalent for the onset of rapid intensification, the individual central-pressure histories of the available sample were checked. Fifty-six of the cases had sufficient consecutive 6-h observations to determine the onset of rapid deepening within 3 h. The majority of the data was collected from the period 1957-1959 and 1966 onward, as late night penetrations were not often conducted during intervening years. Data were biased toward the standard observations of 03, 09, 15 and 21 GMT. The few observations occurring at other times were included with the nearest standard times. A listing of occurrence of the onset of deepening appears in Table 2. For the region considered,

Table 2. Time of occurrence of onset of rapid deepening.

03 (13)	09 (19)	15 (01)	21 (07)	GMT (LST)
10	11	25	10	56 cases
Day (21-03 GMT)			Night (09-15 GMT)	
21 (37.5%)			35 (62.5%)	

the local standard times for Tokyo (140° E) were used (conversion times are indicated in Table 2). The cases were grouped into periods (1900-0100 LST and 0700-1300 LST) to emphasize either day or night periods and to insure that the first 6 h of deepening occurred within one or the other period. The results in Table 2 indicate greater frequencies (35) occurring at night. This suggests that a diurnal

variation might be a contributing feature to intensification.

It is noteworthy that recent studies of rapidly growing tropical oceanic cumulonimbus clouds from satellite imagery (Weickmann et al., 1977) show that pronounced diurnal variation exists in the time of initial development. Maximum frequencies occur near midnight. Observations such as these have not been extended to tropical storms. Studies of tropical storms have been limited so far to analysis of the oscillation of diurnal cloud cover (Browner et al., 1977). One explanation of possible diurnal variations has been offered by Sheets (1969). In his report of mean hurricane soundings, he suggests that differences might exist in the stability of the day vs. night hurricane conditions as a result of diurnal variation of temperature in the middle and upper troposphere. Both Sheets (1969) and Frank (1976) have documented such diurnal variations of temperatures in both hurricanes and typhoons respectively.

4. ASPECTS OF STORM ORGANIZATION

a. Formation period

To gain an idea of organizational time required before commencement of rapid deepening, an evaluation was made of best track analyses for individual typhoons in the Annual Typhoon Reports. Two intensity classifications were considered, including the weak depression stage³ and the point when tropical storm force was first attained.

The data for weak circulation evaluation were limited to 1967 and the years thereafter when routine operational satellite data became available. Analysis of this portion of the cyclone trajectory started often two days prior to aircraft reconnaissance coverage. The aircraft data available in these earlier stages indicated that the central pressures of the tropical cyclones ranged from 1006 to 1008 mb. Forty cases indicating the time elapsed from the weak circulation stage to the onset of rapid deepening were available for study, and the frequency distribution of the various times elapsed arranged into 12 h intervals appears in Fig. 8. The distribution shows predominant frequencies of maximum deepening occurring between 3½ to 4 days following origin. No cases could be identified at 2½ days or earlier. The range included Typhoon Nina (1975) which required only 3 days before entering the stage of explosive deepening (68 mb in 24 h) and Olga

³The JTWC track analysis begins when a weak circulation is identifiable in the cloudiness pattern which is classified as the disturbance stage. A depression classification is not assigned until the circulation has strengthened (25-30 kt) and central pressures have fallen near 1000 mb.

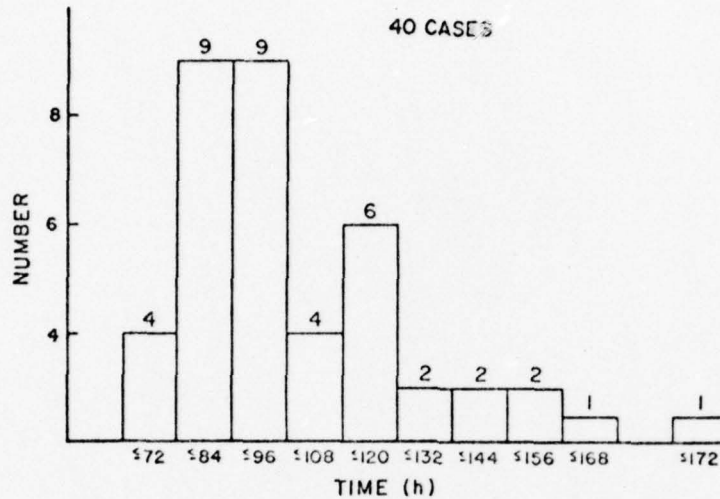


Fig. 8. Time elapsed from origin (weak circulation stage) to onset of rapid deepening.

(1976) which delayed for 8 days until accelerated development took place (46 mb in 24 h).

A mapping of the points first identified for analysis of weak circulation characteristics (Fig. 9) indicates a predominance for longitudes east of 135° E and latitudes equatorward of 15° N. Since circulation systems often move at rates of 9-13 kt, between westerly and northerly headings, the presence of topographical barriers (Philippines, Taiwan) to the west and physical barriers (cooler sea surface temperatures, unfavorable upper tropospheric conditions) dictate a geographical distribution well removed from these influences. (This is discussed further in Section 5c).

Fig. 10 shows a histogram of variations in time elapsed between tropical storm generation and rapid deepening. Of the total sample available, 60 had sufficient data to determine the onset of tropical

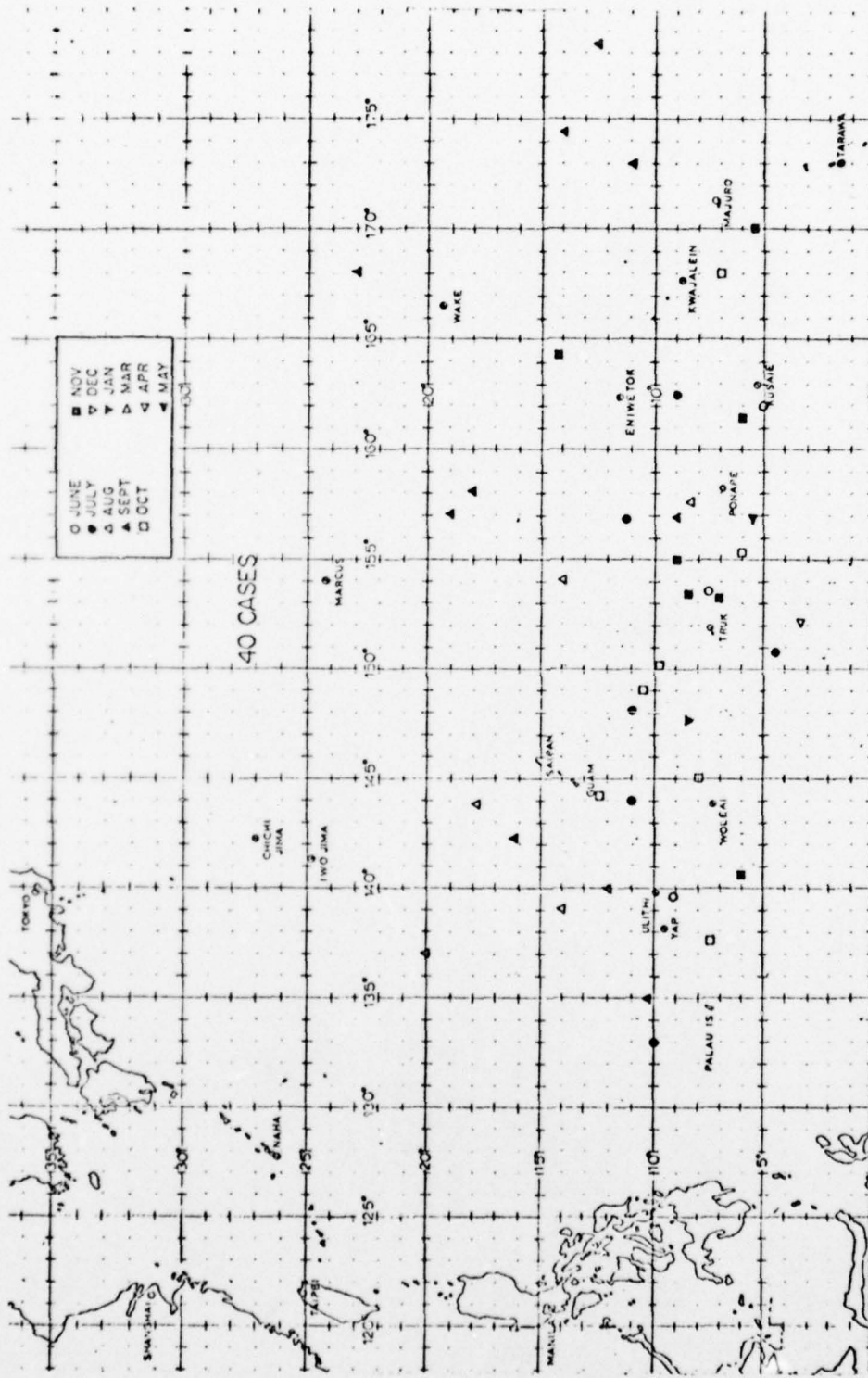


Fig. 9. Origin points (weak circulation stage) of rapid developing typhoons

storm intensity. The central pressure value of 995 mb was selected for a threshold identifier as it corresponds closely with that suggested by the relationship developed by Atkinson and Holliday (1977). As can be noted from the figure, there is a preference for marked intensification between $\frac{1}{2}$ and 2 days after tropical storm generation, as 62% of the cases fall within this interval. Development of type 2 storms characterized the majority of these intensifications. At one extreme both Ida (1969) and Wendy (1963) erupted into sharp pressure falls (61 and 49 mb in 24 h, respectively) within 6 h of tropical storm generation as they traveled slowly near the Marianas. Agnes (1968) and Olga (1976), on the other hand, meandered across the Philippine Sea and took 4 to $4\frac{1}{2}$ days before rapid deepening began.

Of the many numerical simulation models of hurricane intensification developed in the last decade (see Gray, 1975), few have simulated the rapid growth process to meet the criterion established in this paper. Only the model of Kurihara and Tuleya (1974) has reproduced this feature. Their initial maximum wind was assumed at 17 kt with a central pressure of 1006 mb. The circulation strengthened to tropical storm intensity within 42 h and subsequently began deepening rapidly (portraying a type 2 development)⁴ 60 h after initialization. Accelerated growth lasted 24 h during which the central pressure was reduced 57 mb.

Observational evidence shows that relatively few (4) weak circulation systems intensified rapidly in less than 3 d following origin.

⁴A numerical simulation model reproducing type 1 development has yet to be duplicated.

However, an 18-h lapse between tropical storm generation and rapid intensification is realistic (although slightly short of the observational median). Thus, the largest contrast between the model and observations appears to be the shorter time elapsed from initialization in the case of the model. Gray (1975) has commented on the failure of most models (with relatively strong winds, 30-42 kt, at initialization) to intensify within a reasonable time (usual period taken is 3 to 5 d). Comparisons with data in Fig. 10 underscore this

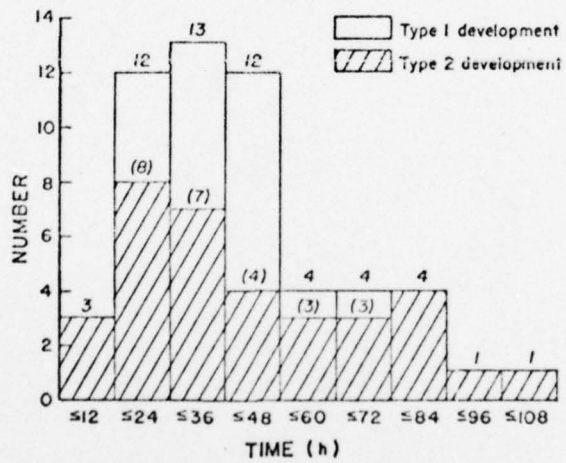


Fig. 10. Time elapsed from tropical storm generation to onset of rapid deepening.

discrepancy, as the bulk of development occurs short of 3 d.

b. Intensity at onset of rapid deepening

Seventy-five of the typhoons were sufficiently documented by reconnaissance observations to allow fairly accurate determination (± 3 h) of the onset of rapid growth. The frequency distribution of central pressure occurring at this time is presented in Fig. 11.

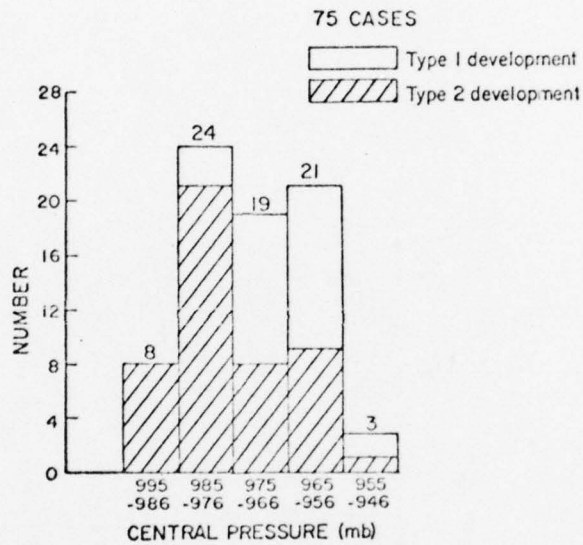


Fig. 11. Frequency distribution of central sea-level pressure at onset of rapid deepening.

The data are segregated into 10-mb class intervals. These data suggest that the majority of the cases of rapid deepening (81%) commenced in the interval 956-985 mb. The variations appear to have a slight biomodal tendency favoring the 976-985 (32%) and the 956-965 mb intervals (28%). The data also show that type 2 development predominates for central pressures of ≥ 976 mb, and type 1 growth becomes more common for lesser pressures. The range of cases varied from Ida (1969)

at 995 mb to Patsy (1973) with 950 mb.

It is noteworthy that the bulk of cases (89%) did not commence rapid deepening until values of 985 mb were reached. This is within one standard error limit of the central pressure (estimated in the Atkinson and Holliday relationship) required to produce typhoon force winds. This pressure threshold has some physical significance. In the western North Pacific as the minimum pressure falls to the vicinity of 980 mb, the radar presentation of the rainbands begins to appear more prominent, thereby displaying a spiral characteristic; and the formation of an eye is often noted at this time. This development in the structure of the rainband activity most often marks the transition from a tropical storm to a hurricane (Dunn and Miller, 1964).

The values of central pressure contained in Fig. 11 were compared to the time typhoon force was first attained. A central pressure of 980 mb was chosen as a threshold mark for determining typhoon intensity for reasons already stated. This value has been used as a similar stratification by Frank (1976) and falls well within the limits of estimate of the Atkinson-Holliday relationship. To minimize the effect of time-interval variations, relative times were rounded to the nearest 12 h. Six typhoons did not have sufficient data and were eliminated from consideration. Fig. 12a portrays the frequency distribution in histogram form and establishes that 62 (85%) of the 73 cases of rapid deepening occurred during the period from 6 h before to 24 h after typhoon generation. The cumulative frequency distribution presented in Fig. 12b shows that the majority (67%) of the rapid deepening had commenced by 18 h after typhoon generation. The range

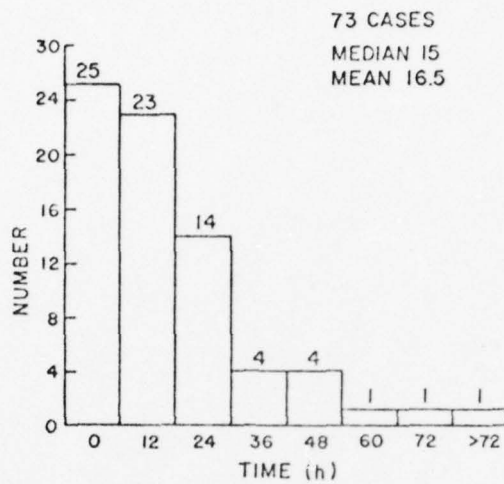


Fig. 12a. Frequency distribution of time elapsing between initiation of rapid deepening and typhoon generation.

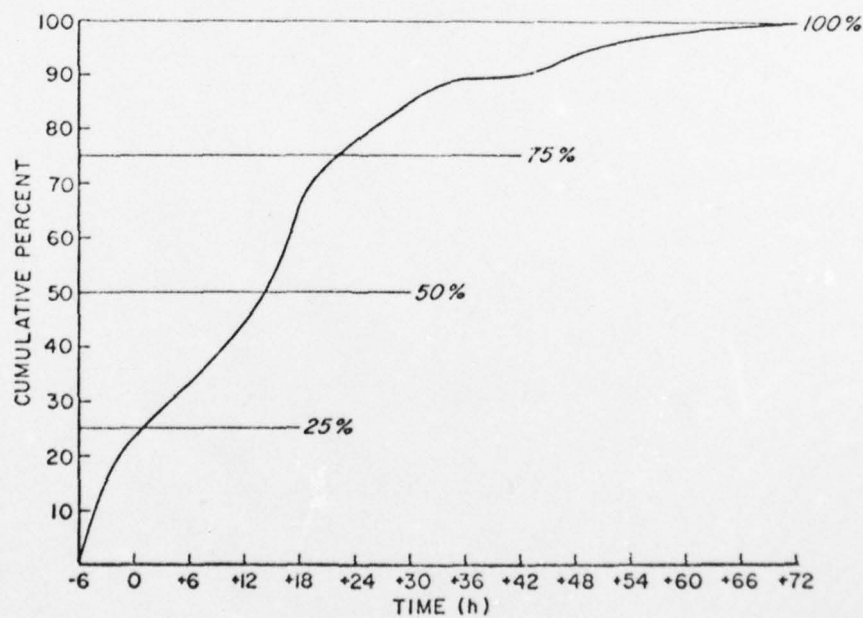


Fig. 12b. Cumulative frequency distribution of time elapsing between initiation of rapid deepening and typhoon generation.

of incidences included Ida (1969) which began a rapid deepening 6 h prior to typhoon onset, and Agnes (1968) which had taken 3½ days after typhoon generation before vigorous development began.

c. Size of eye-cloud wall system

Rapid deepening in close proximity to onset of typhoon intensity is undoubtedly related to the establishment of an eye-wall cloud system at the core of the storm. This system (20-40 n mi radius on the average) constitutes only 1 to 5% of the total storm volume (Centry, 1969); its formation and maintenance, however, play an important role in the intensity of the tropical cyclone. The eye-wall cloud system and its principal surrounding rainbands provide an organizational framework in deep cumulus convection to link the circulations of the tropical upper and lower troposphere for efficient mass transport (Riehl, 1954). As this structure is formed, the onset of sustained hurricane strength winds is usually observed and a more rapid development may commence (Dunn and Miller, 1964).

Several investigators (Jordan, 1961; Colon, 1963; Gray and Shea, 1973; and Bell, 1975) have noted that the smaller the eye-system radius the more efficient is the reduction of central pressure. This is due to a more concentrated action of the storm's thermodynamic engine, thus leading to greater warming by subsidence inside the radius of cumulus activity. In order to determine if rapid deepening occurs with a preferred eye size in the eye-cloud wall system the reports of eye diameter

The diameter information was not included in Annual Typhoon

Reports prior to 1959 and availability of sufficient consecutive 6-h observations in the remaining typhoons further reduced the sample to 42 cases. Most of the eye-diameter observations used were determined from the radar-detected rain-free center and encompassed by $\geq 50\%$ of cloud wall arc. Otherwise the center diameter was measured by the ring of maximum flight-level winds (700 mb or below). Investigations by Shea and Gray (1973) for developed hurricanes have shown that the radius of maximum winds lies just beyond the edge of the rain-bearing clouds (on the average 5 n mi). This discrepancy probably played only a minor role in comparison of observations. In addition, almost all eye observations (37) in the sample were reported circular shaped. The elliptically-shaped eye diameters (5) were obtained by averaging their major and minor axes.

The eye diameter variations observed at the onset of rapid deepening and 12 to 24 h later are presented in Fig. 13. Since eye observations normally were reported in multiples of 5 n mi when > 15 n mi, the class intervals were arranged appropriately. To provide some perspective of the general range of eye diameters and stratification by central pressure, the statistics compiled by Bell (1975) are presented in Tables 3a and 3b.

For the time of onset of rapid deepening, the distribution shows a predominance of cases between 16-20 n mi with a mean of 22.0 n mi and standard deviation of 7.1 n mi. The range is relatively small with no eye diameter larger than 35 n mi and 60% of the cases occurring at diameters of 25 n mi or less. Central pressures at this stage match with Bell's category of 960-979 mb. This grouping possessed a

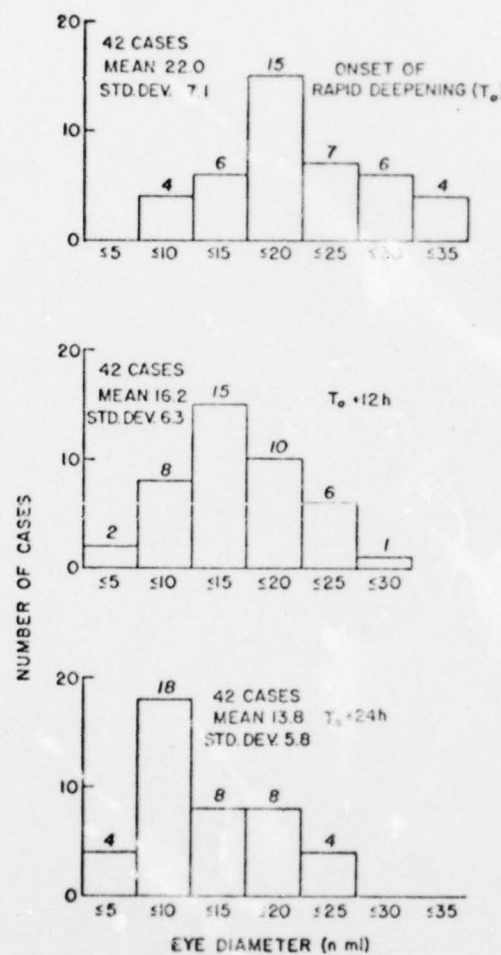


Fig. 13. Frequency distribution of eye diameter at onset of rapid deepening, and 12 and 24 h after t_0 at time.

Table 3a. Frequency distribution of eye diameters for western North Pacific tropical cyclones developing to typhoon force.

Eye Diameter (n mi)	<5	10	20	30	40	50	60	70	80	≥ 85	Total
No. of observations	14	407	586	480	265	104	65	19	37	36	2013
Percentage	7	20	29	24	13	5	3	1	2	2	100%
Average Diameter 27.8 n mi											
Standard Deviation 18.5 n mi											

Table 3b. Same as Table 3a but stratified for central pressure.

Eye Pressure (mb)				
	<920	920-939	940-959	≥ 960
Mean Eye Diameter (n mi)	19.4	24.0	28.4	29.8
Standard Deviation	11.7	10.7	18.1	18.2

mean of 29.8 n mi with 41% of the cases consisting of diameters 20 n mi or less. Thus the comparison suggests a preference for smaller eye diameters than average for rapid deepening. The large diameter eyes (> 35 n mi) appear to be of inadequate dimensions for efficient pressure reduction.

In his study of several Atlantic hurricanes (1958-1961), Colon (1963) suggests that the eye size (radius of maximum winds) during the early stages of hurricane development may influence the intensification rate. The eye vortices of larger diameter (≥ 40 n mi) were noted to be associated with a more gradual intensification than those with a small initial eye size.

Black et al. (1972), in discussing the relatively minor changes in eye size and shape of steady-state hurricanes, remarked that sudden significant changes in eye wall structure usually accompany rapid deepening or filling of a storm. The first situation is clearly demonstrated in Fig. 13, where the mean eye diameter reduces to a smaller size after onset of rapid deepening (22.5 n mi at onset, 16.5 n mi 12 h later, and 13.8 n mi at the end of the period). On the other hand, widening of the eye almost always accompanies filling (Colon, 1963). Some of the most abrupt changes took place in just 6 h from onset of rapid intensification. These included Viola 1969 (20 to 2 n mi) and Elsie 1975 (35 to 10 n mi). Both were reduced to less than 10% of their initial area in a very short time.

5. TRAJECTORY AND SEASONAL--GEOGRAPHIC ASPECTS

a. Trajectory direction and speed

Possible systematic alterations of tracks due to rapid intensification have received little documentation. Dunn and Miller (1964) have cited some observations that the acceleration of a hurricane center is frequently accompanied by intensification. Forecasters also have mentioned that early northward movement of a formative hurricane possibly is related to intensification processes rather than to steering currents (Sugg and Pleisser, 1968). However, Cressman (1952) provides evidence that the areal extent of a developed typhoon is the significant factor for appreciable northward movement because of latitudinal variation of the Coriolis effect across the circulation's diameter.

In order to investigate this subject, the trajectories of 79 sample cases in this study were examined. The tracks of the typhoons were divided into two 24-h segments--one prior to and the other during the rapid growth period. The average 24-h direction was determined by a straight line linking the onset point to the terminal points on the track 24 h before and on that segment after the onset of rapid deepening. This was felt to be more conservative and representative of synoptic-scale mean motion of the storm rather than shorter periods which often may show considerable variability from one 6-h period to another (Jordan, 1963). For the same reason, 24-h averages were used to determine the track speeds. In this case the mean of the four speeds of the 6-h interval was used.

Fig. 14 presents a scatter diagram showing the relation between the direction of mean storm motion during the 24 h before initial intensification time, T_0 , and the direction during the 24 h beginning at T_0 .

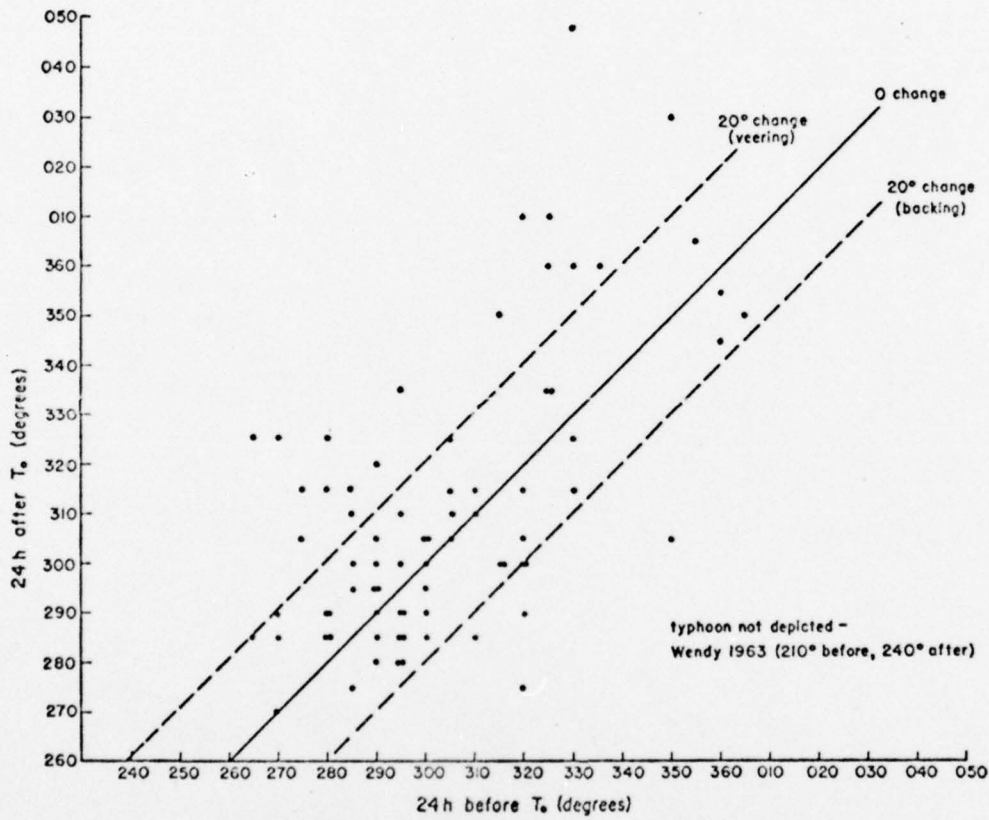


Fig. 14. Mean 24-h direction of typhoon track immediately prior to rapid deepening vs. mean 24-h direction during rapid deepening period.

The majority of cases in each time interval segment fell between the directions of 280° and 310° (57% of these before T_0 , and 53% of cases after T_0). This was not surprising, as another study (Crutcher and

Quayle, 1974) indicated that the directions 290° - 345° are preferred storm tracks at the latitudes considered in this study ($\leq 25^{\circ}$ N). Two storms were somewhat anomalous in direction during their deepening period, namely Wendy (1963) and Faye (1968). Both storms were relatively slow moving (≤ 8 kt), with Wendy directed southwest and Faye heading northeast. This serves as a point of caution against accepting only storms moving from west to north (while south of the subtropical ridge) as candidates for deepening.

Of the typhoons in the sample that eventually recurved into the westerlies (26), none had yet reached the recurvature point before the vigorous growth stage was completed. This is consistent with the findings of Riehl (1972), who examined the intensity of 66 recurving typhoons⁵ (1957-1968) and found all had reached their peak intensity before recurvature.

Almost half (48%) of the directional changes observed were relatively small ($\pm 10^{\circ}$). Of the larger directional shifts ($> 20^{\circ}$), more cases veered (21) after deepening commenced than backed (6). The majority of these (64%) were moving at slow speeds (≤ 8 kt). This behavior is often observed when major track shifts occur. More directional shifts occurred to the right of the previous 24-h track (46) than to the left (28). Such behavior of tracks of tropical storms is well known (Tannehill, 1956; Dunn and Miller, 1964; see also Cressman, 1952).

Fig. 15 portrays a scatter diagram of mean storm speeds 24 h

⁵All typhoons regardless of deepening rate are considered.

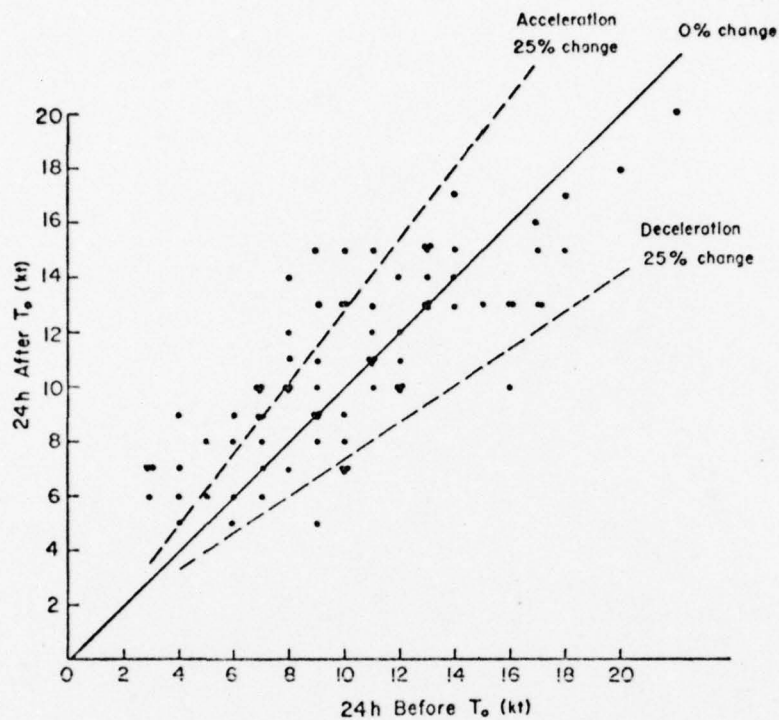


Fig. 15. Mean 24-h typhoon speed immediately prior to rapid deepening vs. 24-h speed during the rapid deepening period.

before significant deepening and during the following 24-h period.

The bulk of the cases (36) before deepening were characterized by moderate speeds.⁶ A slightly lower frequency (28) existed for storms of slow movement, and even less (15) for fast speeds. During the deepening period, the majority of the cases (40) tracked at moderate rates, with a near equal number at both slow (21) and above normal speeds (18). The range of the speeds (5-20 kt) spanned about the

⁶To classify relative rates, categories of slow (≤ 8 kt), moderate (9-13 kt), and fast (≥ 14 kt) were chosen as defined by Shea and Gray (1973).

same interval as those prior to deepening. The difference between the two time periods showed only a minor increase in the mean of 1 kt (9.9 before to 10.9 kt after). The median speed remained at 10 kt for both periods.

An examination of individual changes in speed indicated that there were more cases of accelerating (39) than decelerating (28) systems. Twelve storms displayed no change in speed of movement. The majority of typhoons (56) showed changes \leq 25% of the 24-h speed immediately before rapid development. A greater number of accelerations $>25\%$ (18) were noted than decelerations (5). These accelerations, however, did not result in speeds greater than 11 kt. Of the individual cases, the most notable change in speed occurred during Typhoon Joan which was approaching the Philippines at a rate of 16 kt and decelerated to 10 kt (31% change) during the deepening period. At the other extreme, Typhoon Trix (1960) moved at 9 kt during the first 24-h period preceding intensification and accelerated to 15 kt (66% change) during the intensification. By contrast, Typhoon Nora (1973) deepened some 69 mb in the Philippine Sea with little or no change in forward speed observed.

No prevalent relationship appears evident in speed or speed changes in cases of rapid deepening. In summary, however, it is interesting to note an apparent tendency in Fig. 15 for storms traveling faster than normal to decelerate during the deepening process while those initially moving at slow speeds display a gradual acceleration.

b. Seasonal distribution

The annual distribution of rapid deepening is presented in Fig. 16. As no surprise, it indicates that this phenomenon occurs during July through November, the main months of the typhoon season. However, the data point out that rapid deepening is not confined to these months, but several occurrences have been recorded in the winter and spring seasons. Incidents of extreme deepening (≥ 60 mb in 24 h) also have been included for comparison and are noted to be most prevalent during September and October. Values are given at the bottom of the figure for the percentage of rapid deepening as compared to total monthly frequency.⁷ November is seen to have the highest percentage with the months July-October having nearly equal frequency. The minimum noted for August by Brand (1973) for typhoons intensifying more than 50 kt in 24 h is not apparent in these data.

A breakdown of the most active part of the year into 15-d periods⁸ as displayed in Fig. 17 is somewhat more revealing of the seasonal distribution. The bulk of cases is confined to summer and early fall (76%). Activity began in the last part of June (all cases were confined to the last week), increased during late July through August, and peaked between mid-September and mid-October. An absence of any activity was noted during the last 15 d of October (Ida, 1969

⁷Based on average frequency per month from data compiled by JTWC for period 1959-1976 (1976 annual typhoon report). Months must have at least 30 typhoons for comparison, thus resulting in exclusion of winter and spring months.

⁸Thirty-one day months have last day included in latter 15-d period.

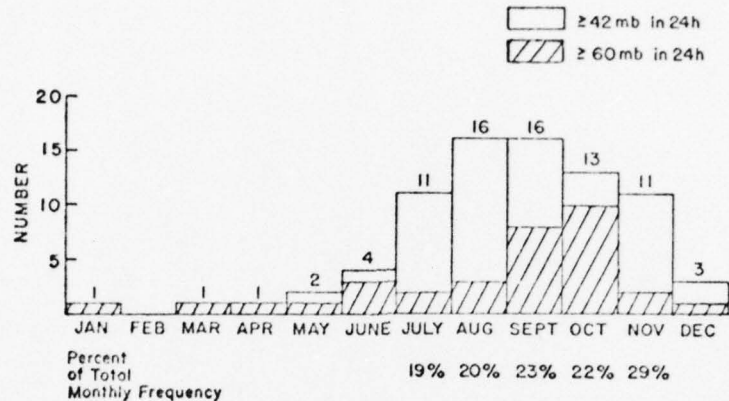


Fig. 16. Annual distribution of rapidly deepening typhoons (1956-1976).

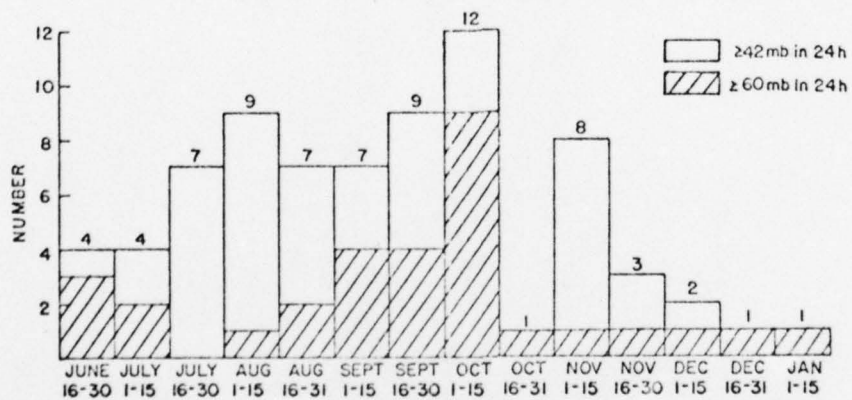


Fig. 17. Distribution of rapid deepening during main activity period by $\frac{1}{2}$ month periods).

occurred on the 16th), which served as a convenient point to demarcate the main season. Activity reappeared during the first of November but tapered off sharply thereafter. The most striking period of activity occurred during the first part of October, when 13 storms were recorded, 10 of them of the extreme variety (≥ 60 mb in 24 h). Combining the period 16 September through 15 October, we see that the peak of annual activity is represented for both rapid (21) and extreme (13) deepenings.

c. Geographic distribution

The geographic distribution of locations where typhoons intensified rapidly is shown in Figs. 18 and 19. The data were divided as suggested by the seasonal frequency. Fig. 18 shows the summer and early fall (20 June - 16 October) and Fig. 19 shows the remainder of the year. The midpoints of the track segments were identified, and the latitude and longitude of these points were averaged for each 5° Marsden square to represent the centroid of the points contained in the square. Isopleths of these values were drawn to highlight areas of highest activity (Figs. 20 and 21).

The summer-early fall situation (Fig. 20) portrays a large majority of all occurrences concentrated in a 5° band between 15 and 20° N beginning some 300 n mi east of Luzon and stretching eastward to the vicinity of the northern Marianas. In contrast to the Philippine Sea, the South China Sea is almost free of rapid growth cases. This was not unexpected as typhoons that form in the South China Sea often reach landfall before they can intensify significantly.

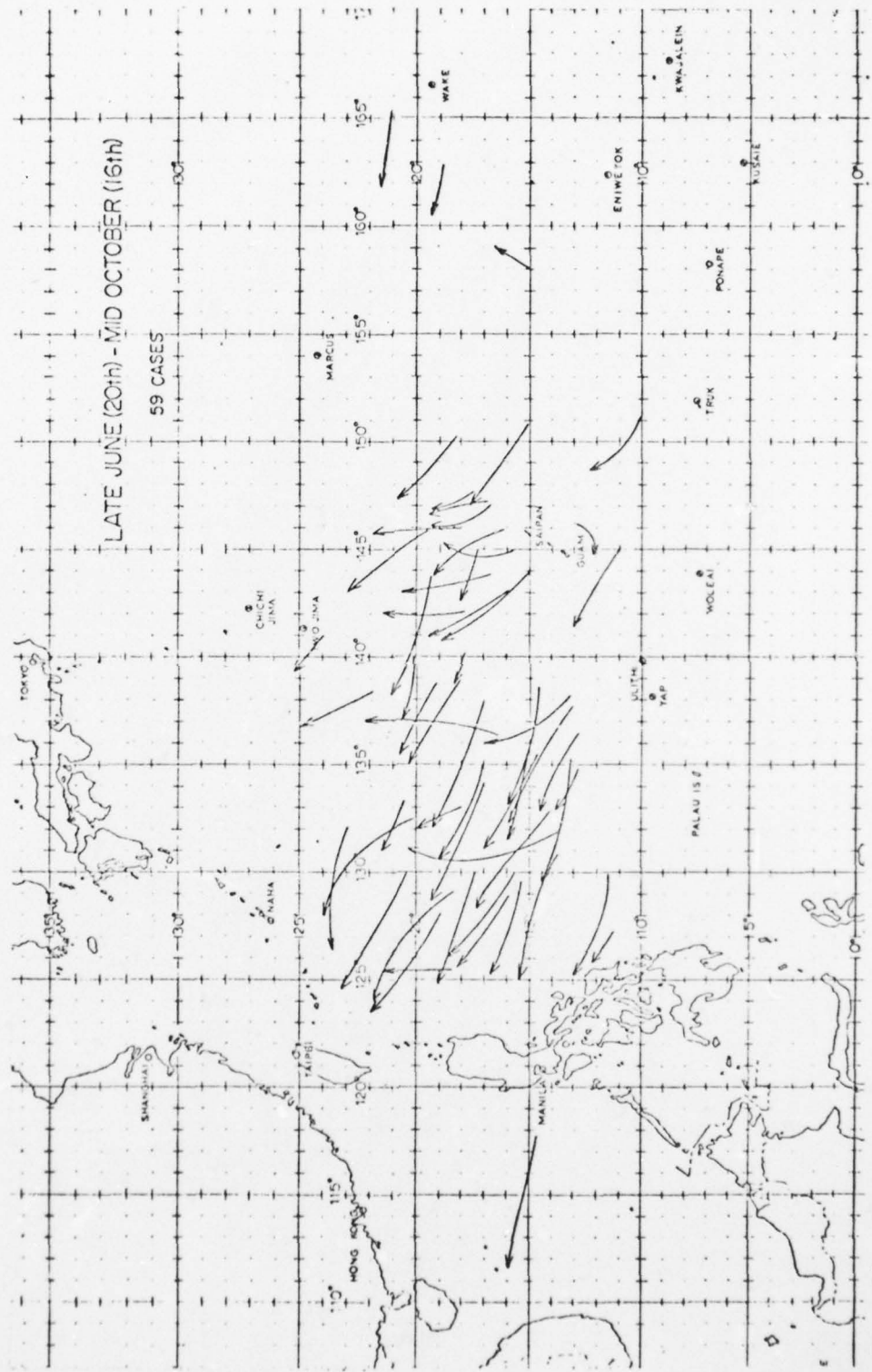


Fig. 18. Typhoon track segments (1956-1976) for period of rapid deepening (24 h) during summer and early fall (20 June-16 October).

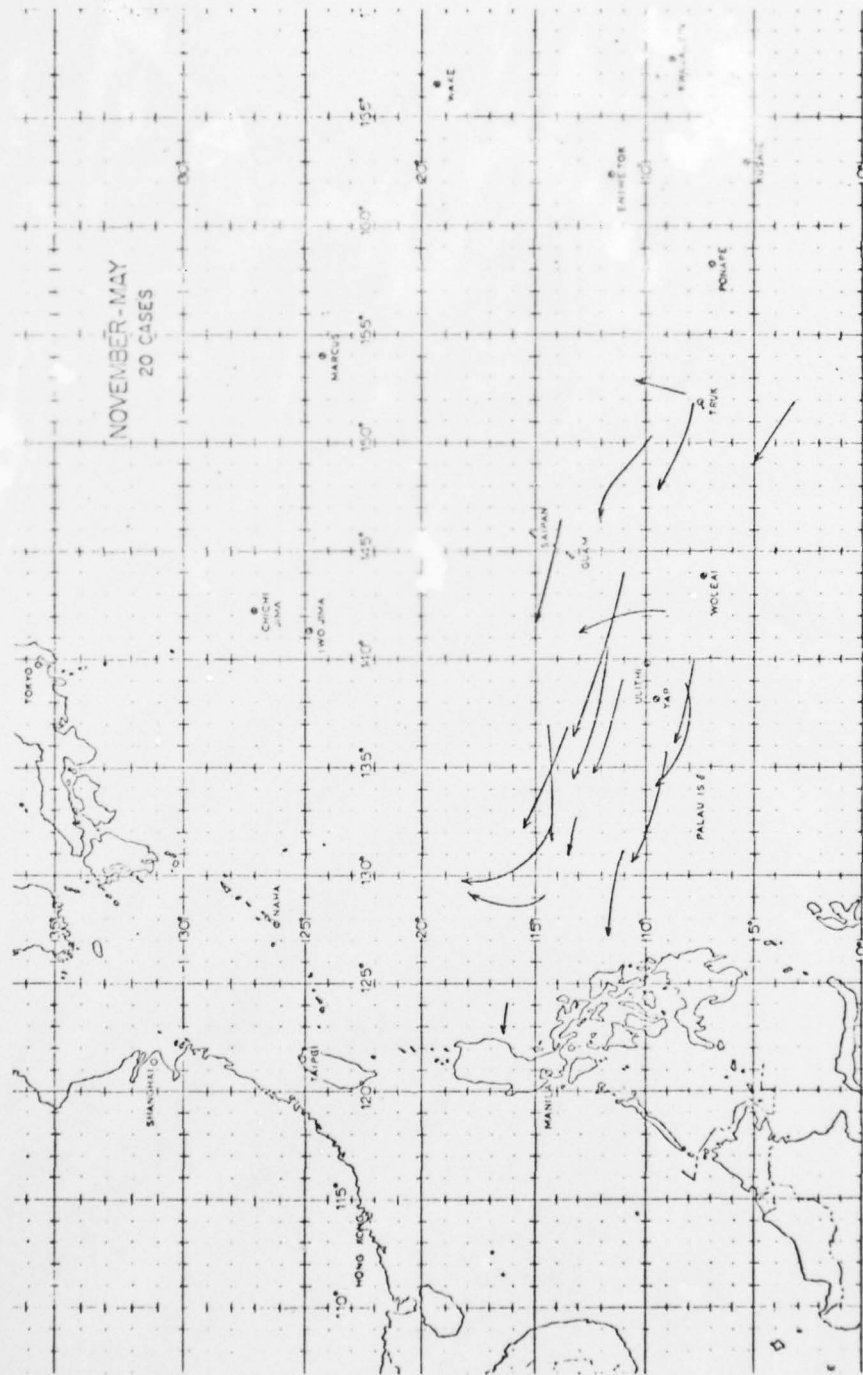


Fig. 19. Typhoon track segments (1956-1976) for period of rapid deepening (24 h) during late fall through spring (November-May).

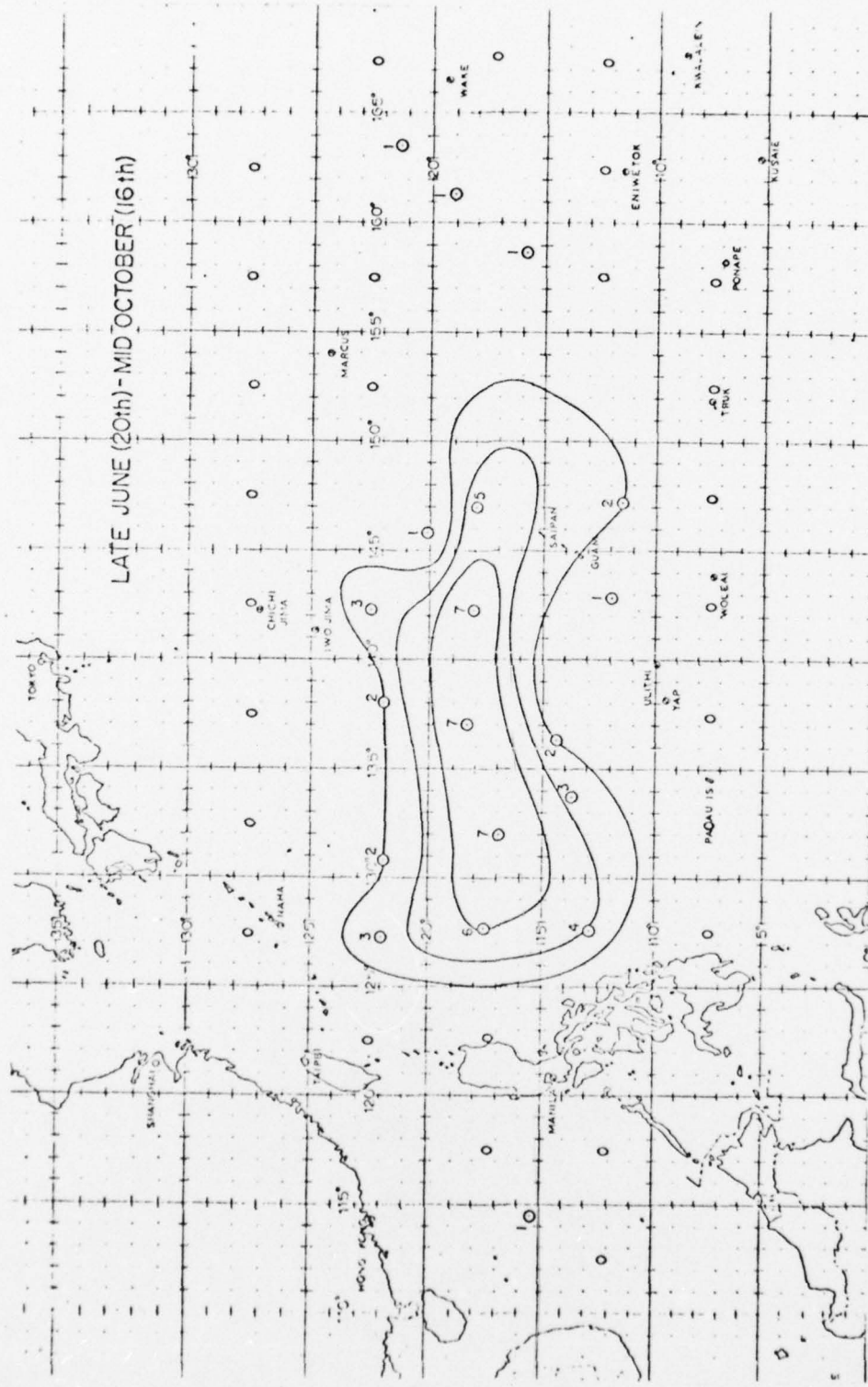


Fig. 20. Areas where typhoons intensified rapidly during summer and early fall (20 June-16 October)
—number of occurrences (1956-1976).

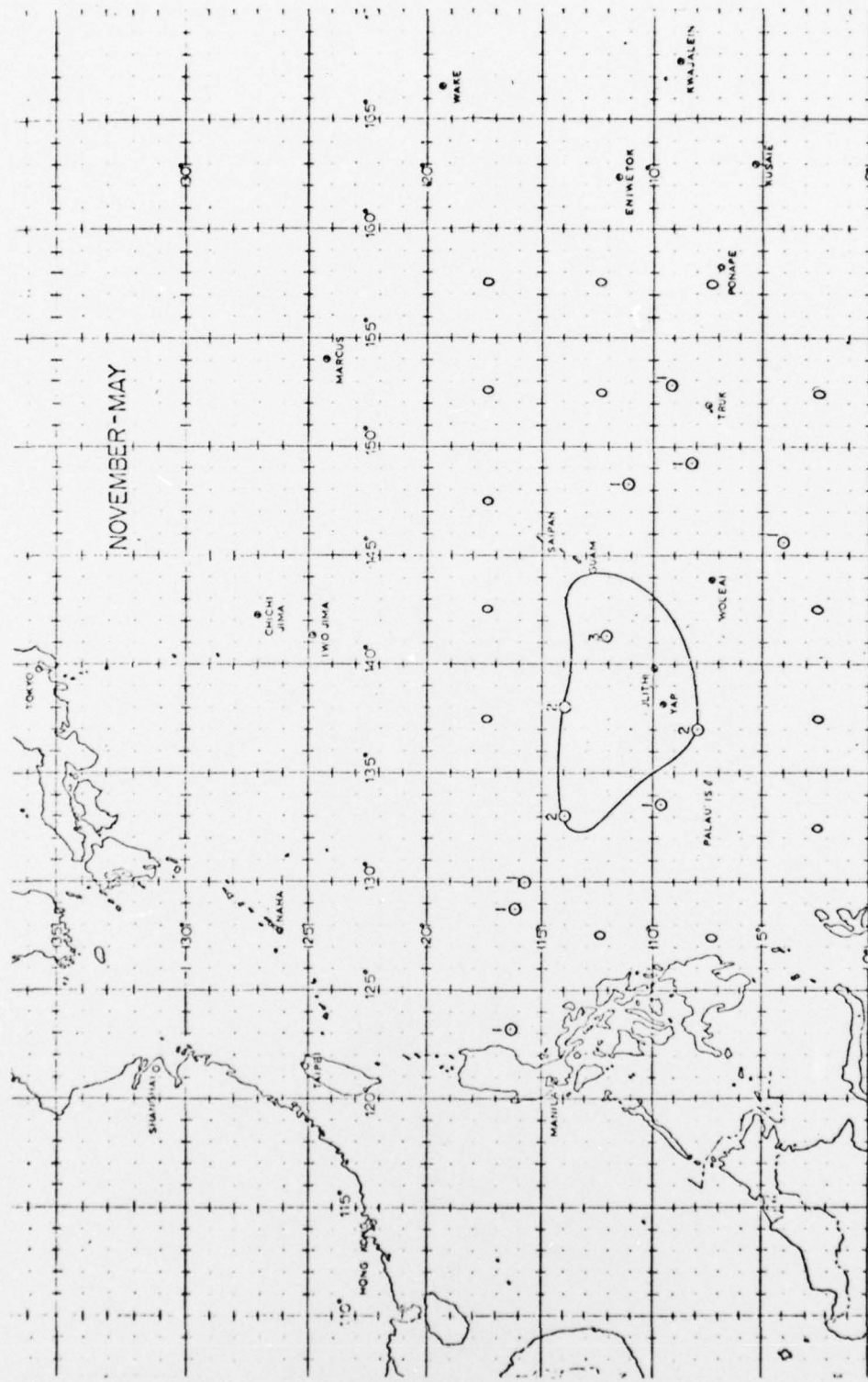


Fig. 21. Areas where typhoons intensified rapidly during late fall through spring (November-May)
—number of occurrences (1956-1976).

Those storms that enter from the Philippine Sea are weakened as their circulations are disrupted by the rough terrain of the Philippine Archipelago. Once regeneration occurs over the open sea, it is a relatively short time before landfall on the Indo-China Peninsula or southern China. The relatively few occurrences east of the Marianas are primarily the result of the normal absence of the low-level monsoon trough in this region. Eighty-five percent of all typhoons generate within the monsoon trough (Gray, 1975). Those typhoons that do develop in this region are initiated by disturbances associated with upper tropospheric lows and account for the remaining 15%; few if any such cases become well developed.

During the late fall through spring, (Fig. 21) the preference for development has shifted 5° equatorward and is concentrated in the latitude belt between $10-15^{\circ}$ N. The maximum is not as longitudinally spread, being displaced further eastward from the Philippines and limited by the southern Marianas. Surges of the northeast monsoon dominate the area east of Luzon with cooler dry air during November through early spring (Ramage, 1971) thereby presenting a hostile environment for additional development of storms that migrate to this region. Favorable conditions for storm maintenance northeast of Luzon usually do not return until late spring when the southwest monsoon becomes established. This was the case for Olga, 1976, which was stalled off the coast in the later part of May.

1) Ocean temperature influence

The tropical cyclone gains its energy from the ocean and also

tends to be more intense where sea-surface temperatures are the highest (Miller, 1958). In an attempt to explain the geographical distribution of rapid deepening, the sea-surface temperature was examined over the region for each typhoon intensification in the sample. Ten-day marine sea-surface temperature charts prepared by the Japanese Meteorological Agency were inspected to determine the temperature prior to arrival of the typhoon⁹—so that the temperature would not be influenced by strong winds of the storms and subsequent upwelling of cooler water. With the data available, the period of record studied was 1959–1976.

Table 4 shows the frequency of temperatures at commencement and termination of rapid deepening. The majority of cases were confined

Table 4. Sea-surface temperature variation associated with rapid deepening (1959–1976)—62 cases.

Temp °C	<u>Cases</u>	
	<u>Onset</u>	<u>Termination</u>
26 to 26.9	0	0
27 to 27.9	1	2
28 to 28.9	15	19
29 to 29.9	43	38
30 to 30.9	3	3

⁹Although local sea-surface temperature may vary over just a few days, the 10-d sea-surface temperature should provide sufficient information as the tropical cyclone circulation covers a relatively large area.

to values of 28-29° C. This corroborates the findings of Ito (1963) who found rapid deepening (2.0 mb h^{-1}) of typhoons (1954-1960) associated with sea-surface temperatures of 28° C or greater. Few times, if any, did the temperature in the present sample reach the theoretical values required for deep storms (30-31° C, central pressure $\leq 914 \text{ mb}$) as advanced by Miller (1958).

Several investigators including Perlroth (1967) and Leipper and Volgenau (1972) have emphasized the importance of considering not only the surface temperature but also the temperature of the upper ocean layer. Should only a shallow layer of warm water exist, than the large surface energy requirement for sustaining a rapidly intensifying typhoon may not be met. A study by Jordan and Frank (1964) indicates that a mixed layer depth of some 30 m is required to prevent cold water mixing from below. Gray (1975) has given attention to an increased depth of 60 m in assessment of ocean thermal potential for tropical cyclone genesis.

In order to examine this aspect, a climatological approach was necessary, as vertical depth measurements of the upper ocean layer are not routinely available in advance of a typhoon. An atlas of monthly subsurface ocean temperature compiled by Robinson and Bauer (1971) was consulted and values at 30 m and 60 m extracted at points where rapid deepening began and terminated. Table 5 presents the results for the 62 typhoons examined earlier for surface temperatures. Almost all showed high temperatures of $\geq 28^\circ \text{ C}$ to 30 m. However, cooler temperatures often were in evidence at the 60-m levels. Climatologically, these data would suggest a mixed layer depth of $\geq 28^\circ \text{ C}$

Table 5. Subsurface climatological temperature variation associated with rapid deepening (1959-1976)—62 cases.

Temp °C	30 m depth (cases)		60 m depth (cases)	
	<u>Onset</u>	<u>Termination</u>	<u>Onset</u>	<u>Termination</u>
23 to 23.9	0	0	0	2
24 to 24.9	0	0	0	1
25 to 25.9	0	0	2	1
26 to 26.9	0	0	1	8
27 to 27.9	0	3	8	20
28 to 28.9	13	31	27	20
29 to 29.9	49	28	23	10

to 30 m as a limiting criterion for rapid development.

Figs. 22 through 27 display the climatological locations of the mean monthly 28° C isotherm for sea surface, 30-m and 60-m depth based on the atlas of Robinson and Bauer (1971). Track segments of rapidly intensifying typhoons occurring within the month are also mapped. With the exception of Anita (August 1970), Thelma (August 1962), and Helen (September 1964), all tracks terminated at or equatorward of the 30 m isotherm. Thus the climatological location of the 28° C isotherm at 30 m depth might, in part, explain the poleward limit (and western demarcation line in the South China Sea) of the geographical distribution of storms displaying rapid growth¹⁰.

¹⁰Several storms such as Ellen, (July 1973), Mary (July 1971) and Trix (August 1971) began rapid development ($\geq 1.75 \text{ mb h}^{-1}$) poleward of this limit. However in each case the trend was a short one (6-12 h).

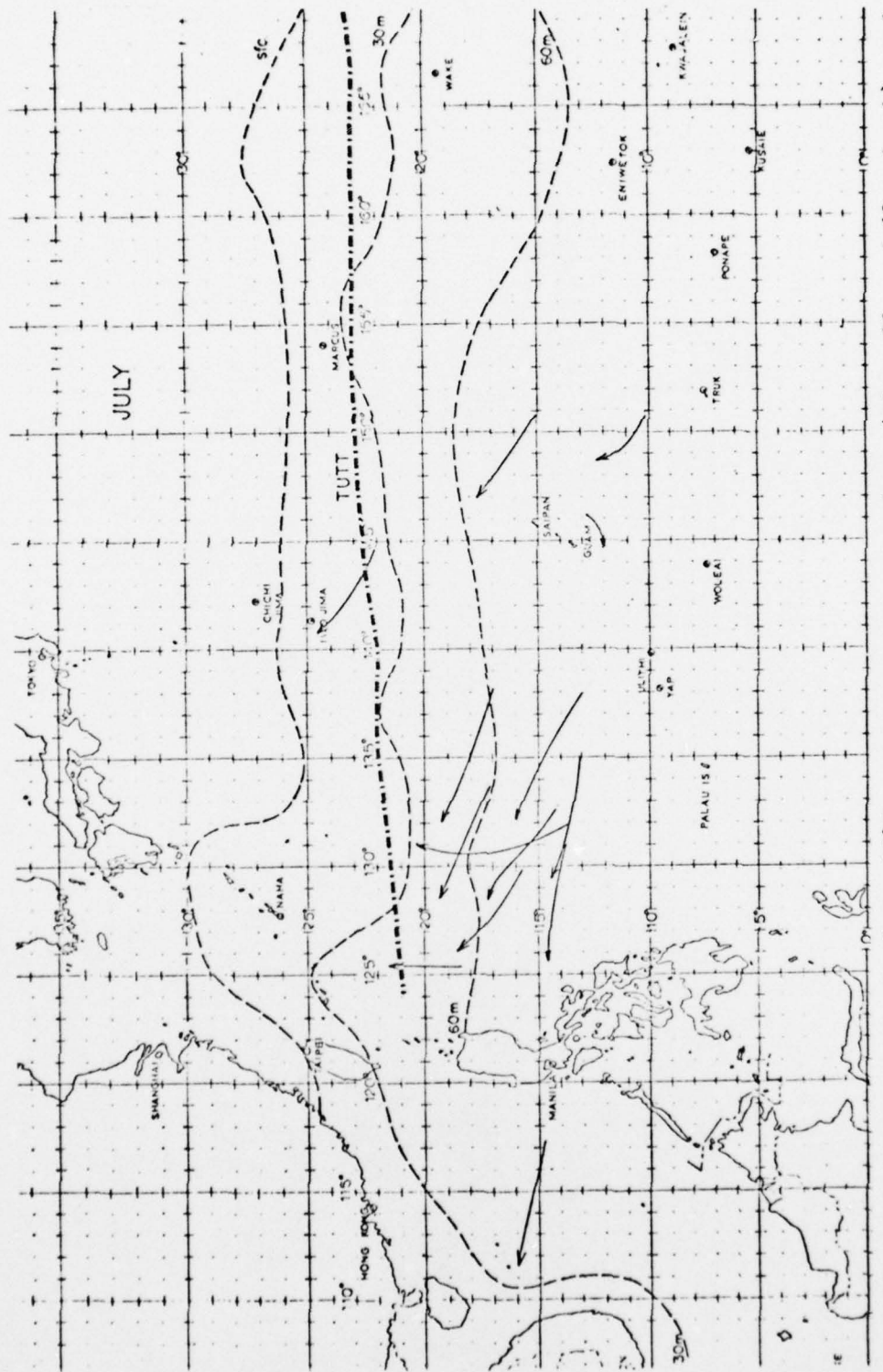


Fig. 22. July mean positions of the 28°C ocean temperature isotherm (sfc., 30-, and 60-m depth), and the 200-mb Tropical Upper Tropospheric Trough (TUTT). Typhoon track segments denoting period of rapid deepening for both June (last week) and July are indicated.

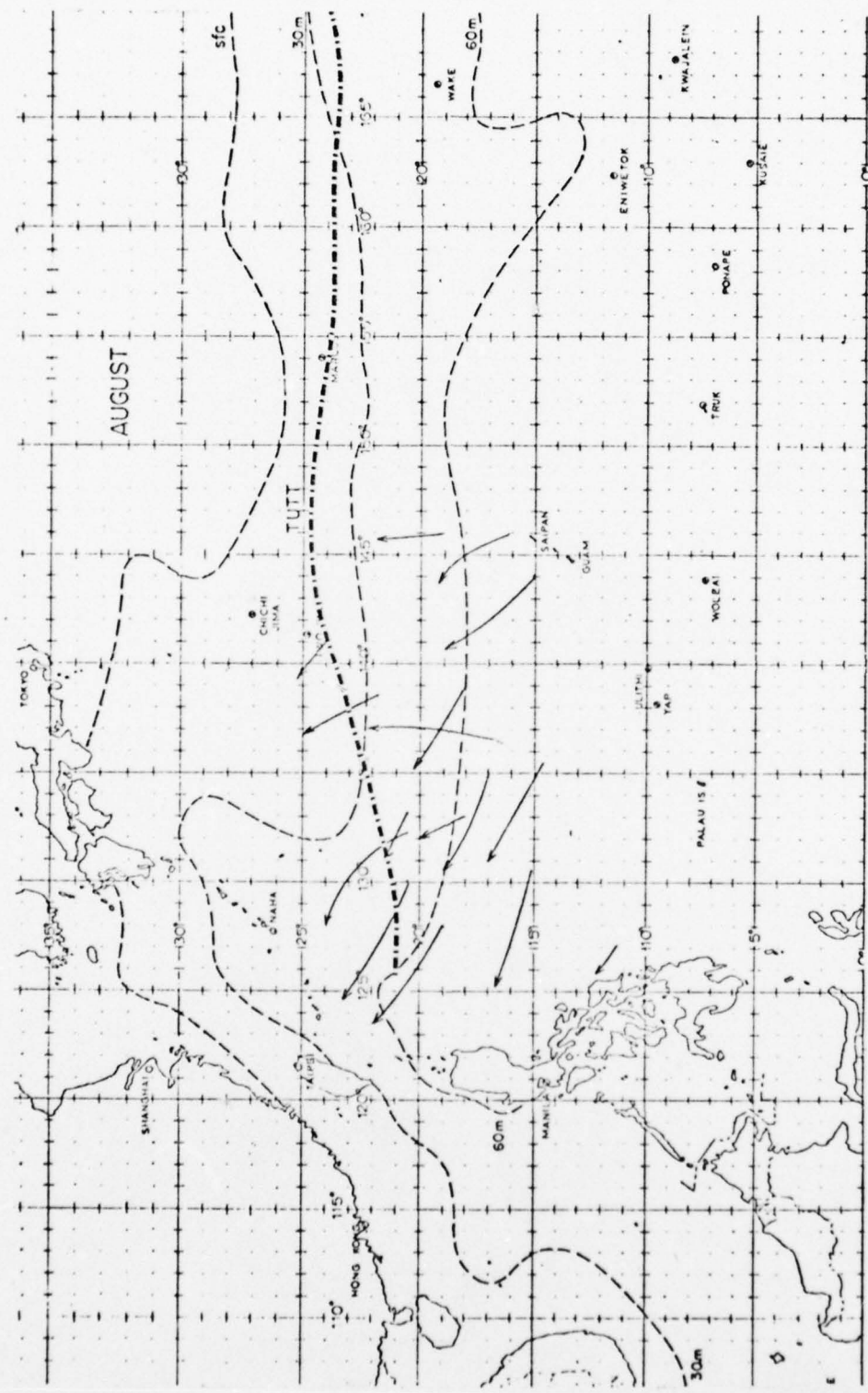


Fig. 23. August mean position of the 28°C ocean temperature isotherm (sfc., 30-, and 60-m depth), and the 200-mb Tropical Upper Tropospheric Trough (TUTT). Typhoon track segments denoting period of rapid deepening for August are indicated.

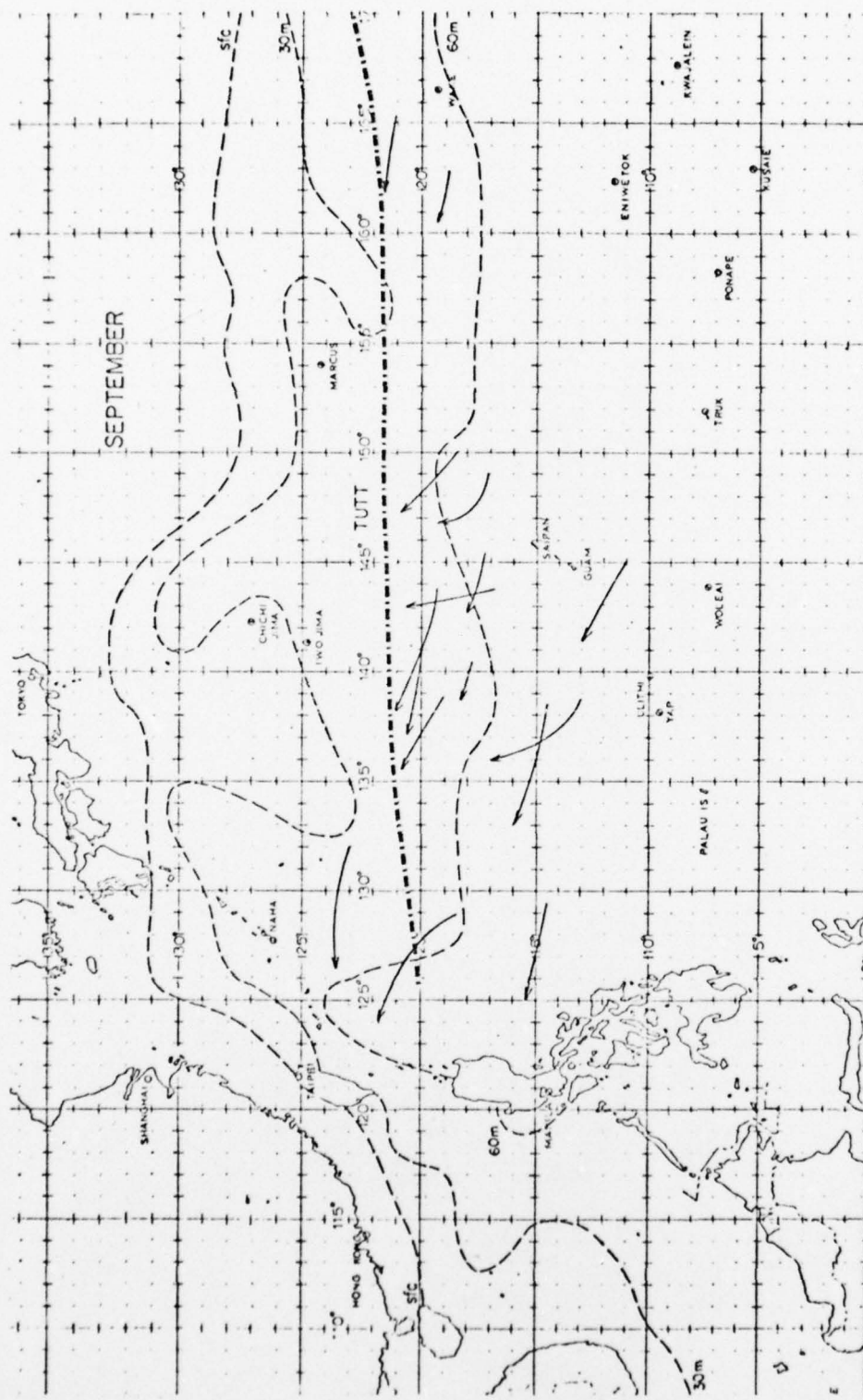


Fig. 24. September mean position of the 28°C ocean temperature isotherm (sfc., 30, - and 60-m depth), and the 200-mb Tropical Upper Tropospheric Trough (TUTT). Typhoon track segments denoting period of rapid deepening for September are indicated.

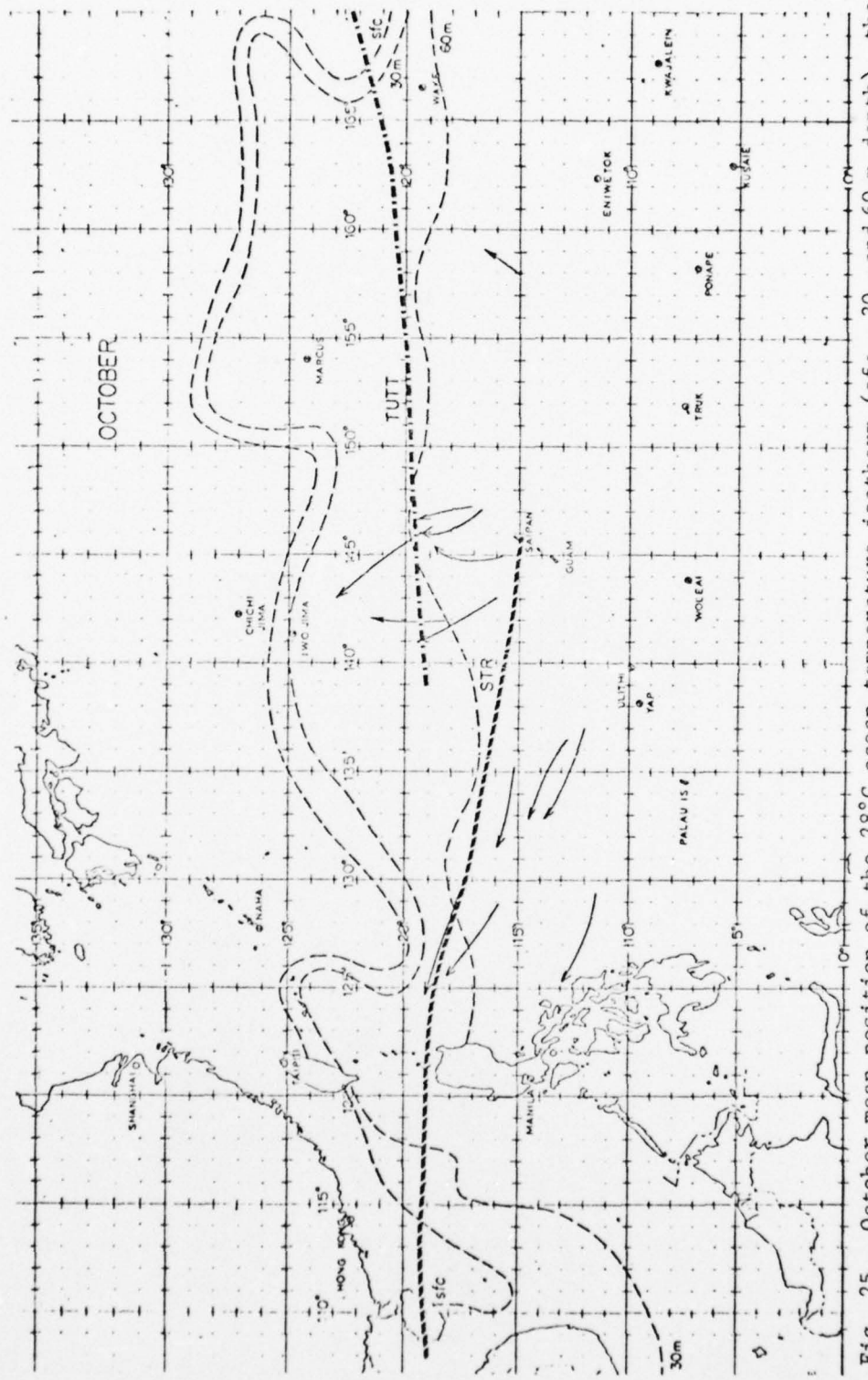


Fig. 25. October mean position of the 28°C ocean temperature isotherm (sfc., 30-, and 60-m depth), the mean position of the 200-m Subtropical Ridge (STR), and the average position (between September and October) of the Tropical Upper Tropospheric Trough (TUTT). Typhoon track segments denoting period of rapid deepening for October (all within first 16 d) are indicated.

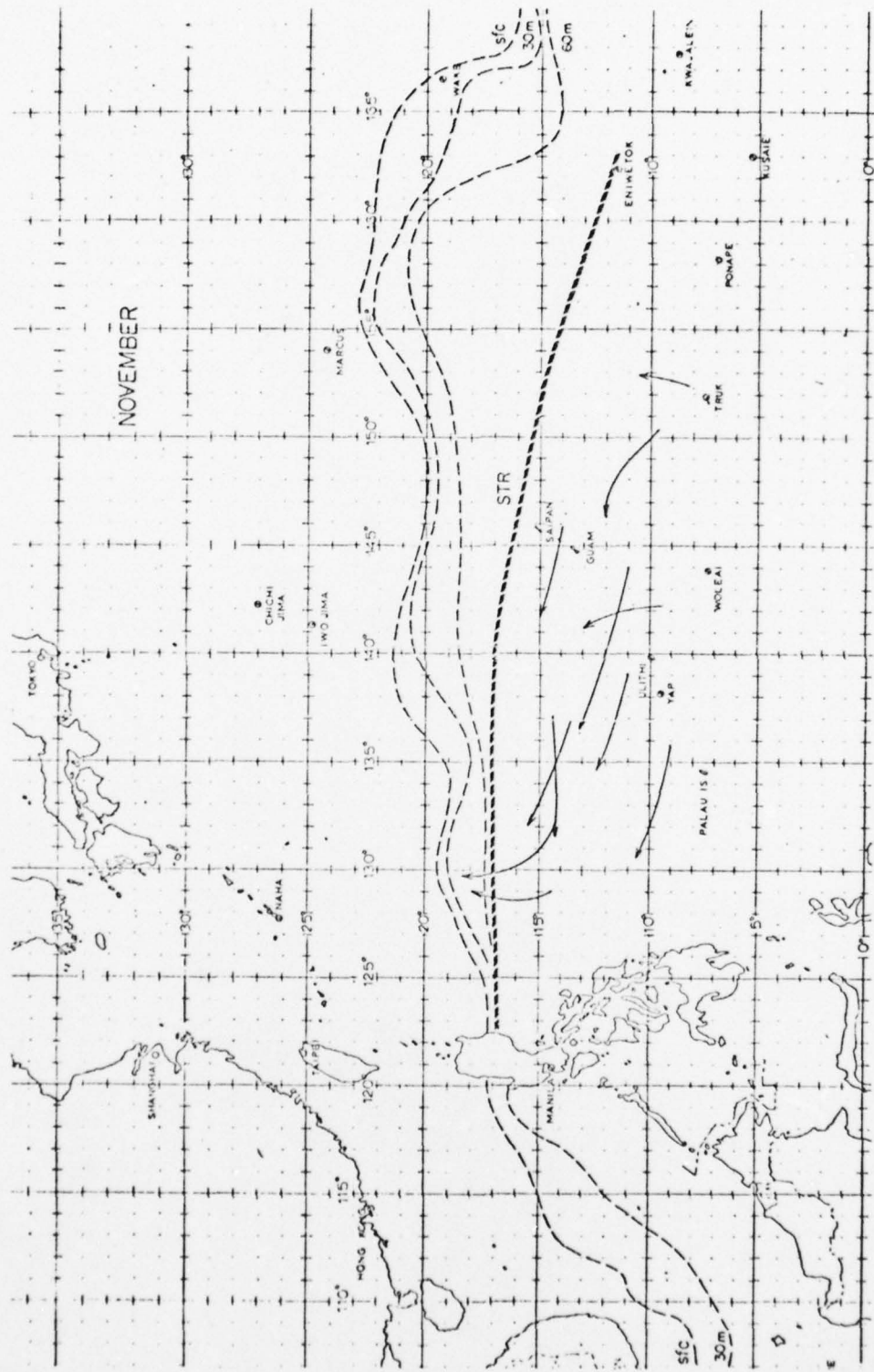


Fig. 26. November mean position of the 28°C ocean temperature isotherm (sfc., 30- and 60-m depth), and the 200-mb Subtropical Ridge (STR). Typhoon track segments denoting period of rapid deepening for November are indicated.

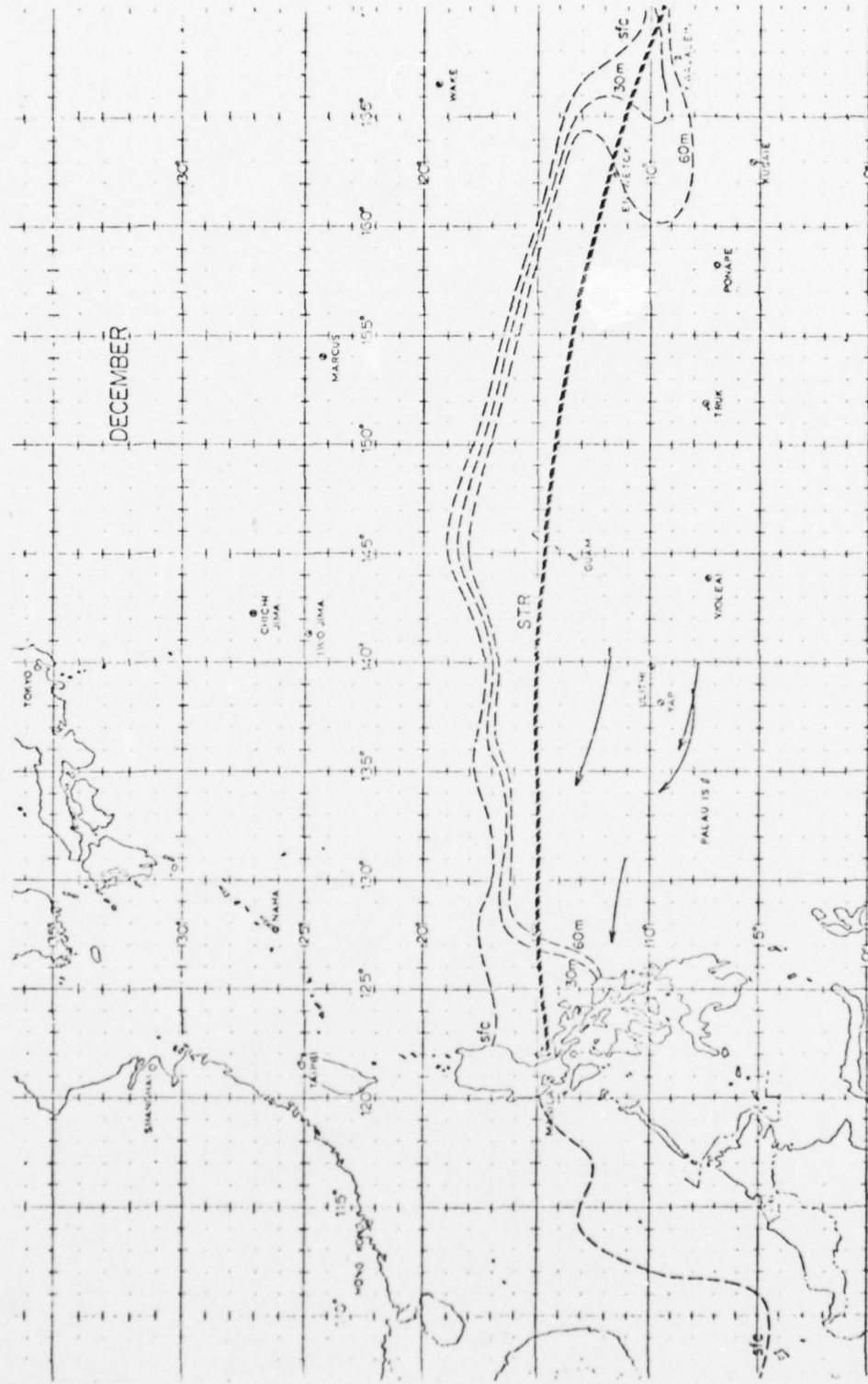


Fig. 27. December mean position of the 28°C ocean temperature isotherm (sfc., 30,- and 60-m depth), and the 200-mb Subtropical Ridge (STR). Typhoon track segments denoting period of rapid deepening for December and the first week of January are indicated.

However, ocean temperature influences can be considered only as a necessary but not sufficient condition for abnormal intensity growth. The bulk of the typhoons traversing these warm waters displayed only normal development and many weakened (Brand, 1973). It is evident that upper tropospheric circulation features play the significant role (Ramage, 1974).

2) Upper tropospheric influences

Upper tropospheric outflow to the westerlies in the northern sector of a tropical cyclone has long been recognized as a requirement for hurricane development (Riehl, 1954; Dunn and staff, 1964; Colon and Nightingale, 1963). Deep troughs in the westerlies can often facilitate this flow during the late fall and spring. However during the summer and early fall troughs in the mid-latitude westerlies seldom extend into the tropical western North Pacific (Sadler, 1976a). The circulation feature that provides a westerly channel for outflow during this period of the year is the Tropical Upper Tropospheric Trough (TUTT), a feature first identified by Ramage (1959) as important for typhoon development.

Fig. 29 depicts a schematic (from Sadler 1976a) of storm outflow interaction with larger scale circulations in the upper troposphere. Fig. 28a portrays a model view of outflow into the subtropical westerlies enhanced by a deep mid-latitude trough while outflow equatorward is directed into the easterlies. [This semi-permanent feature of increasing speed westward (due to the easterly jet) provides a persistent outflow mechanism from the storm's

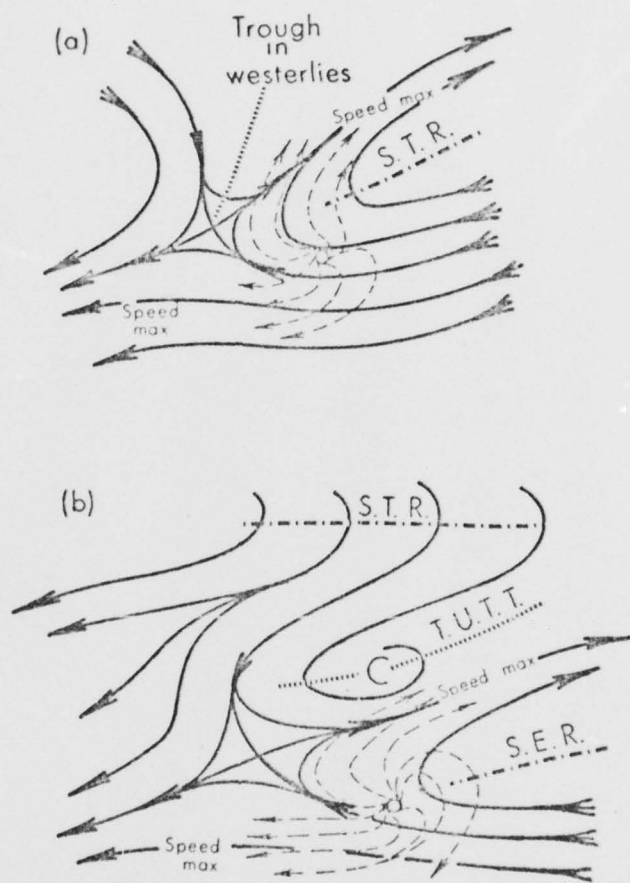


Fig. 28. Schematic of storm outflow interaction (dashed lines) with the larger scale circulation (solid lines). STR is the Subtropical Ridge; SER, the Subequatorial Ridge; and TUTT, the Tropical Upper Tropospheric Trough. (from Sadler, 1976a)

equatorial flank during the summer and fall]. Fig. 28b portrays the interaction of the storm outflow with the Tropical Upper Tropospheric Trough (TUTT) and the resultant channel into the westerlies.

The TUTT's specific role in enhancing development and influencing intensity changes has been documented recently by Sadler (1976a, 1976b). In view of the foregoing evidence, it is of importance to consider this feature when examining geographic distribution of rapid deepening.

The monthly climatological positions of the TUTT as determined from an atlas of 200-mb circulation over the tropics prepared by Sadler (1975) have been marked on Figs. 24-27. It is noted that the poleward limit of rapid deepening occurs within $\pm 2^\circ$ of latitude of the TUTT during these months. In essence, for those typhoons that move poleward of these latitudes, the trough reforms south of the typhoon thus effectively cutting off equatorward flow to the easterlies with concurrent termination of the intensification.

Fig. 29 and 30 present satellite imagery examples. Typhoon Betty (12 August 1972) in Fig. 29 is an intensifying storm (center located near 18° N 138° E); outflow is occurring in the northern sector to the east with cloudiness equatorward of the typhoon indicative of outflow into the easterlies. On the other hand, Typhoon Anita (20 August 1970) is shown in Fig. 30 (center located near 28° N 136° E) with a clear zone equatorward of the typhoon, indicative of the presence of an upper-level trough blocking outflow equatorward into the easterlies. Anita's central pressure was filling at this time.

By the early part of October subtropical westerlies prevail east of the Asian continent, and the TUTT retreats eastward and disappears

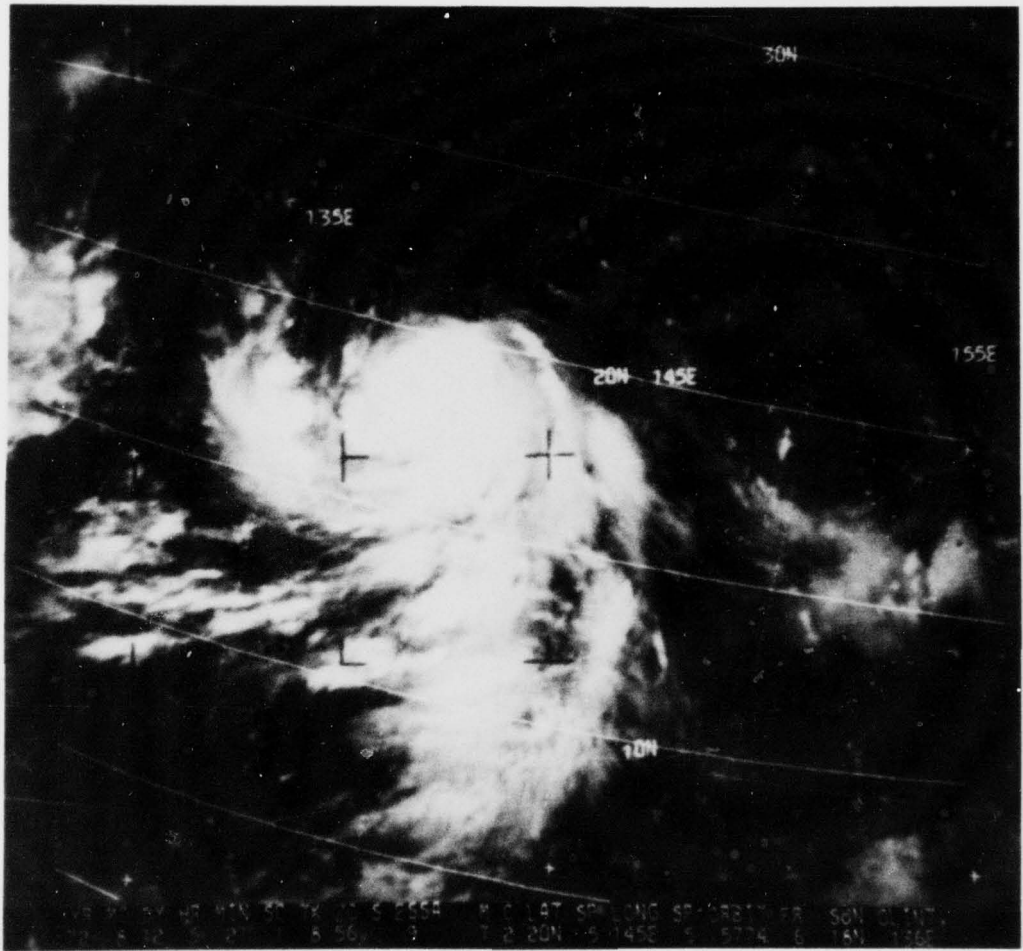


Fig. 29. ITOS-1 satellite view of typhoon Betty (12 August 1972) with cloudiness features south of the typhoon depicting outflow into the upper tropospheric easterlies.

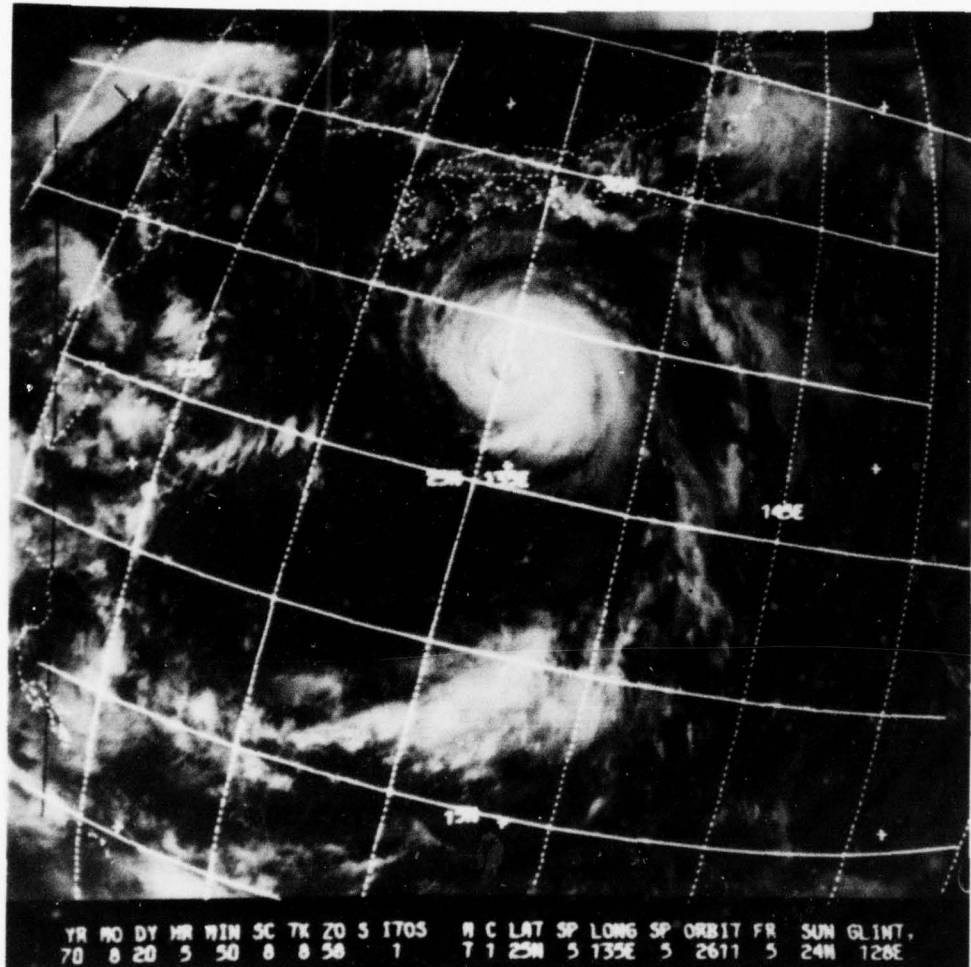


Fig. 30. ITOS-1 satellite view of typhoon Anita (20 August 1970) with cloudiness absent equatorward of the typhoon indicating outflow to the upper tropospheric easterlies has been severed.

later in the month. The 200-mb subtropical ridge becomes the latitudinal brake as suggested by the track segments in Figs. 25-27. Poleward of this position, equatorial flow is severed and the storm system is subjected to increasing magnitudes of vertical wind shear (Gray, 1975). This demarcation line persists through the winter and spring until reestablishment of the TUTT in early summer. A slight seasonal preference appears in the geographic distribution of rapid deepening from summer to fall. This also has been noted by Brand (1973). In late June through August (Figs. 22 and 23), there is a tendency for most of the tracks to be located in the western portion of the Philippine Sea, while during September and early October (Figs. 24 and 25), trajectories are confined more to the eastern portion. The meridional orientation of the tracks suggests that deep mid-latitude troughs are beginning to appear during the latter period thereby preventing more westerly movement. Development through processes shown in Fig. 28b is thus common in these situations.

Although climatological features may be used to explain, in part, the geographic distribution of rapid deepening, recognition of the individual case with respect to particular upper tropospheric patterns is necessary if prediction skill is to be realized.

6. OUTFLOW CHARACTERISTICS

a. Introduction

The upper tropospheric circulation has a critical role in determining a typhoon's intensity. This was best emphasized by Sadler (1976a, 1976b), who showed that the presence of multi-directional outflow channels plays an important part in the development of tropical cyclones in the near-equatorial surface trough. Dvorak (1975) has observed in satellite imagery studies that cirrus clouds spreading out from tropical cyclones in three or more quadrants are indicative of both typical and rapid development. Forecasters, including the author of this work, also have remarked on the existence of several avenues of outflow into the large-scale circulation often attendant with marked intensification. Characteristics specific to the rapid deepening case, however, have not been addressed, and discussion of general features has been largely qualitative. Thus, the effort in this section will be to describe quantitatively the preferred outflow characteristics associated with rapid development on a more quantitative basis.

To focus on the most significant features of upper tropospheric outflow from intensifying typhoons, two sets of contrasting rates of development were selected. One set consisted of ten explosive deepening cases (≥ 60 mb in 24 h). The other, used for comparison, included slow to normal deepening typhoons (≤ 24 mb in 24 h).

b. Data discussion

The period 1970-1975 was selected for study since upper tropospheric (200-mb) data and daily operational satellite imagery were readily available for these years. A list of the typhoons chosen during the period is given in Table 6. With the exception of one storm (Patsy, 1973) all extreme deepening typhoons occurring during the period are represented. The map time closest to (but before) the onset of rapid deepening was chosen for analysis. Criteria for the selection of typhoons in the comparison set showing non-rapid intensification were based on deepening rate, intensity and geographical position. This required development profiles less than the median normal (≤ 24 mb in 24 h) central pressures supporting typhoon velocities (≤ 980 mb), center position equatorward of 22° N latitude and at least 30 h from landfall.

To form the data base for the analysis of these selected storms, charts prepared by the JTWC primarily were utilized (period 1971-1975). These maps contained data from several sources including standard rawinsonde observations, transient aircraft Doppler winds (within 6 h of synoptic time) observed between heights of 10 and 12 km, and wind directions determined by cirrus cloud plumes observed in high resolution satellite imagery (Defense Meteorological Satellite Program; see Meyer, 1973). For the earlier year (1970), upper-air charts containing similar data and produced by Fleet Weather Central, Pearl Harbor, Hawaii, were utilized also. However, cloud direction elements determined from satellite imagery had to be added (Environmental Survey Satellites of the U.S. Department of Commerce).

Table 6. Typhoons Selected for Analysis.

a - Extreme Deepening (≥ 60 mb per day)						
Typhoon	Date-Time (GTT)	Latitude ($^{\circ}$ N)	Pressure (mb)	Central	Previous	Fall
				24 h Fall	(mb per day)	24 h Later
Olga	30 June 70 - 00	9.0	964	28		60
Hope	23 Sep 70 - 00	18.5	974	24		81
Joan	11 Oct 70 - 12	11.5	978	15		62
Amy	01 May 71 - 00	8.0	970	25		70
Irma	11 Nov 71 - 00	12.5	968	19		95
Billie	14 July 73 - 00	18.5	985	18		65
Nora	04 Oct 73 - 12	13.0	968	10		72
Nina	01 Aug 75 - 12	20.5	969	26		69
Elsie	11 Oct 75 - 00	17.5	973	17		69
June	18 Nov 75 - 00	9.5	965	15		89

b - Slow or Normal Deepening (≤ 24 mb per day)						
Typhoon	Date-Time (GTT)	Latitude ($^{\circ}$ N)	Pressure (mb)	Central	Previous	Fall
				24 h Fall	(mb per day)	24 h Later
Lola	01 June 72 - 00	11.0	977	14		18
Alice	02 Aug 72 - 12	17.5	974	17		9
Helen	14 Sep 72 - 00	18.5	970	20		10
Ida	19 Sep 72 - 12	10.5	970	5		4
Marie	07 Oct 72 - 00	15.0	964	10		13
Olga	26 Oct 72 - 00	14.0	976	15		13
Gilda	02 Jul 74 - 00	19.5	971	19		11
Polly	28 Aug 74 - 00	20.0	964	26		15
Elaine	26 Oct 74 - 12	17.0	980	23		24
Irma	24 Nov 74 - 00	14.0	974	10		17

Fig. 31 (for Typhoon Hope, September 1970) displays a typical distribution of data. Both streamline and isotach fields were analyzed from the mapped data with emphasis placed on continuity and interpretation of meteorological satellite imagery (see Sadler, 1976a) where conventional data were absent. It might be noted that investigations by Frank (1976) have shown that the maximum outflow level is located near 150 mb for typhoons. However, Black and Anthes (1971) have remarked that cirrus motion may not occur at the level of maximum outflow. Thus, considering the data analyzed, it is quite possible that velocity magnitudes obtained may not be at the level of maximum wind.

In order to evaluate the outflow characteristics, an analysis of radial wind components at selected radii was used. A stationary grid of 15° latitude radius and positioned on the typhoon center (geographic references; North - 360°) was employed. The grid consisted of five radial bands (5°, 7½°, 10°, 12½°, and 15°) with increments of 30° tangential extent about each band. Radial components of the wind measured at 60 grid points per storm were evaluated by graphical methods. No attempt was made to obtain measurements within 5° of the typhoon center due to the usual unavailability of data. The 5° circle also serves as a convenient limit marking the extent of the mean typhoon circulation scale (Frank, 1976). An outward limit of 15° radius was considered sufficient to include the major upper tropospheric circulation influences interacting with the typhoon outflow.

The average radial wind component at each of the data points were

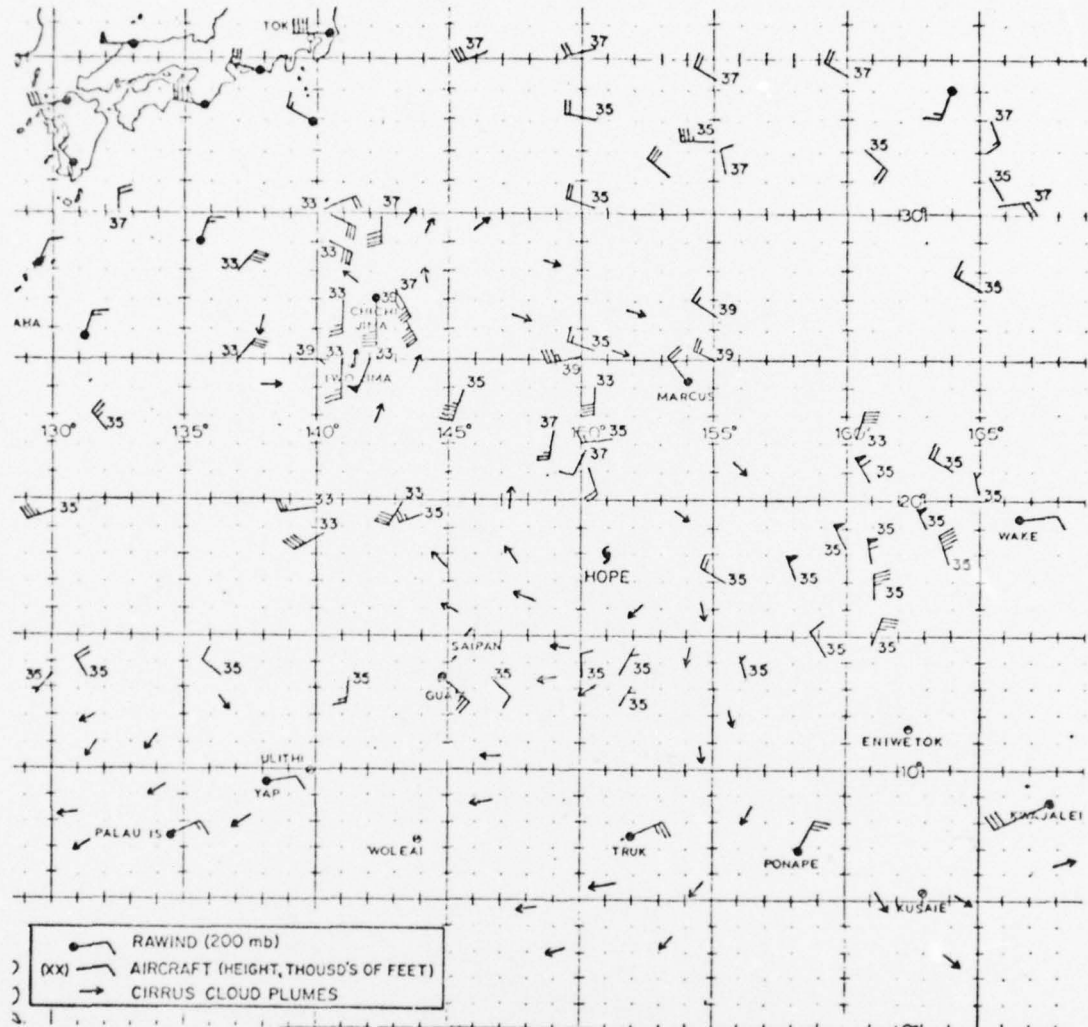


Fig. 31. Upper tropospheric data typically available for analysis, including conventional rawinds, transient aircraft Doppler measurements, and flow direction derived from cirrus clouds depicted in satellite imagery. (Typhoon Hope, 0000 GMT 23 September 1970.)

used to form an average wind field for all data points for both the rapid intensification group and the more slowly developing cases. The composite charts pertaining to the two growth-rate types are presented in Figs. 32 and 33. In addition a listing of sector preference for outflow was compiled for each typhoon (Table 7). Only radial winds with magnitudes of ≥ 7 kt for each data point between radius bands 5° to 10° were counted.

c. Results

Typhoon intensification outflow characteristics, as observed by Sadler (1976b), are an upper tropospheric channel to a large-scale westerly flow, in addition to the normally available channel to the large-scale easterlies. For the extreme deepening cases studied, this was the most prevalent characteristic of interaction of the typhoon with surrounding circulation patterns. The composited data bear this out, as Fig. 32 shows magnitudes of radial wind component ≥ 15 kt towards the northeast and east as well as towards the southwest.

Slower developing storms also were observed to exhibit outflow (≥ 15 kt) to the easterlies due to the persistent nature of this climatological feature (Fig. 33). However, exhaust to the north was frequently restricted by the close proximity (within 5° of latitude) of the Tropical Upper Tropospheric Trough (TUTT). The associated equatorward flow about the subtropical ridge and into the TUTT accounts for radial inflow in the northeast quarter. In addition, at the 5° radius, the slower developing storms often exhibited little

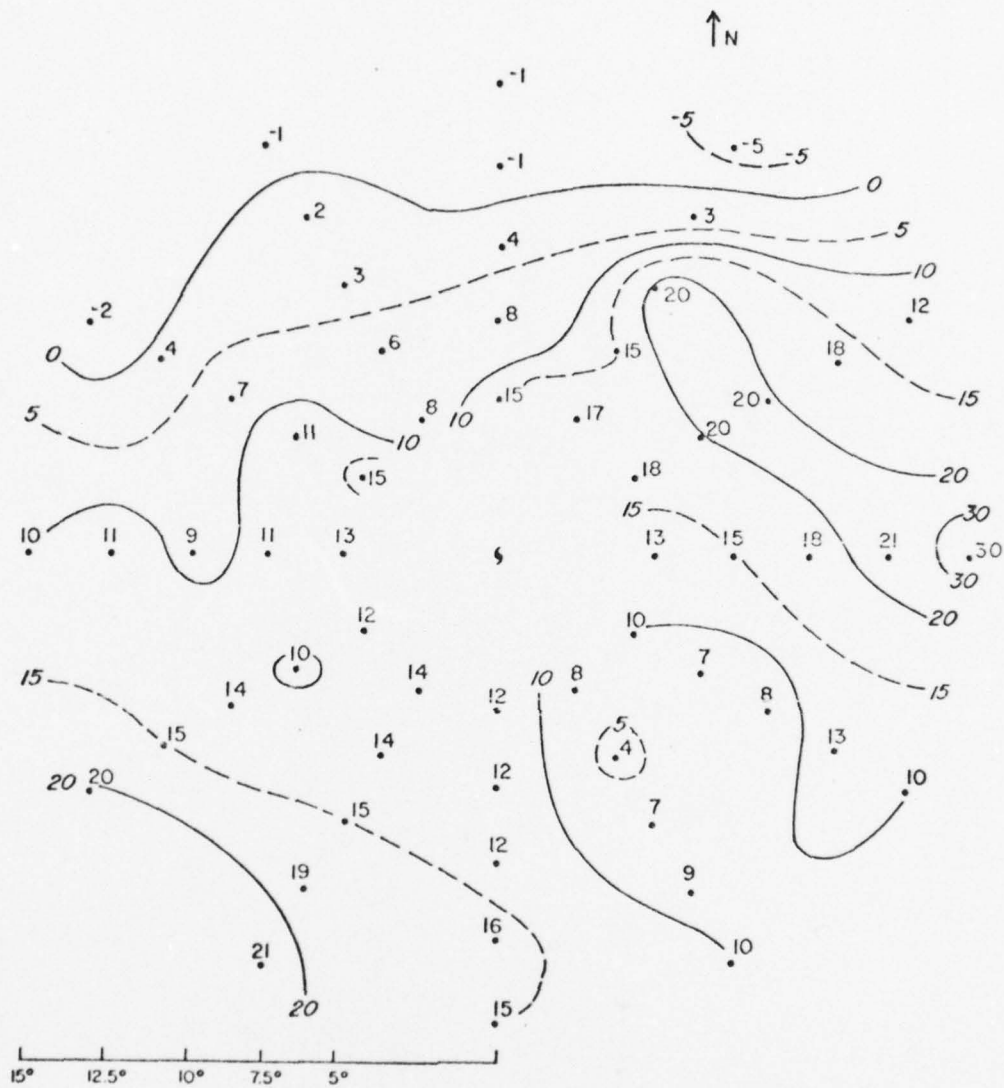


Fig. 32. Composite 200-mb radial wind component field for ten extreme deepening typhoons (≥ 60 mb in 24 h).

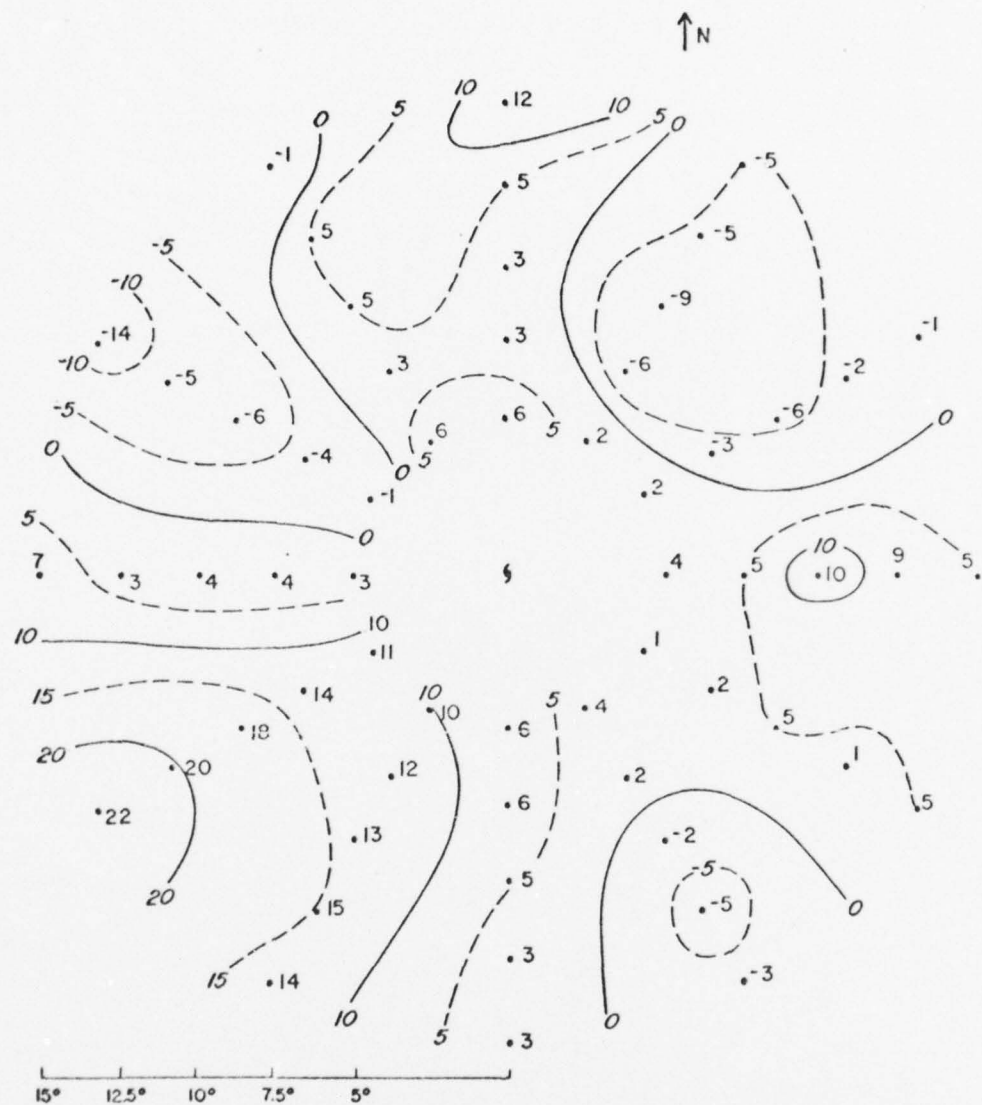


Fig. 33. Composite 200-mb radial wind component field for ten slow to normal deepening typhoons (≤ 24 mb in 24 h).

Table 7. Preferred Outflow Sectors, 5-10° from Center
(outward radial component ≥ 7 kt for each data point)

Typhoon (Yr)	360	30	60	90	120	150	180	210	240	270	300	330	Total Radials	
													Showing Outflow	
a. Extreme Deepening (≥ 60 mb per day)														
AZIMUTH (Degrees)														
Olga (70)	x	x	x	x	x	x	x	x	x	x	x	x	x	x
Hope (70)														
Joan (70)	x	x	x	x	x	x	x	x	x	x	x	x	x	x
Amy (71)	x	x	x	x	x	x	x	x	x	x	x	x	x	x
Irma (71)	x	x	x	x	x	x	x	x	x	x	x	x	x	x
Billie (73)	x	x	x	x	x	x	x	x	x	x	x	x	x	x
Nora (73)	x	x	x	x	x	x	x	x	x	x	x	x	x	x
Nina (75)	x	x	x	x	x	x	x	x	x	x	x	x	x	x
Elsie (75)	x	x	x	x	x	x	x	x	x	x	x	x	x	x
June (75)	x	x	x	x	x	x	x	x	x	x	x	x	x	x
Mean	0.5	0.8	0.8	0.9	0.4	0.1	0.8	0.8	0.6	0.4	0.5	0.3		7.1
b. Slow or Normal Deepening (≤ 24 mb per day)														
AZIMUTH (Degrees)														
Olga (72)	x	x	x	x	x	x	x	x	x	x	x	x	x	x
Lola (72)	x	x	x	x	x	x	x	x	x	x	x	x	x	x
Alice (72)														
Helen (72)														
Ida (72)														
Marie (72)														
Olga (72)														
Gilda (74)	x	x	x	x	x	x	x	x	x	x	x	x	x	x
Polly (74)	x	x	x	x	x	x	x	x	x	x	x	x	x	x
Elaine (74)	x	x	x	x	x	x	x	x	x	x	x	x	x	x
Irma (74)	x	x	x	x	x	x	x	x	x	x	x	x	x	x
Mean	0.4	0.1	0.1	0.4	0.1	0	0.4	0.6	0.6	0.2	0	0	0	3

outflow in their eastern sectors, and their circulations frequently were nearly concentric in this region, thereby indicating little interaction with the large scale.

Several typhoons of the slower developing group, however, exhibited contrasting behavior, as outflow to the southwest was absent and outlets to the north through east were in evidence. These typhoons either were cut off by troughs from interacting with the monsoon easterlies (Alice 1972; Lola 1974; Polly 1974) or occurred in a period when the easterlies normally are weak [Irma 1974 (late November)]. One of the vigorously developing storms also did not display outflow towards the southwest (Elsie 1975), as an upper tropospheric cold low blocked any spread of exhaust in that direction. The low did, however, enhance the typhoon's outflow about its northern flank toward the west and contributed to the storms intensification.

Evidence of an outlet to the northwest was apparent in half the extreme deepening cases. Typhoon Hope (1970) was an exception with a radial component to the outer grid ring. This was caused by an upper tropospheric cold low in the region which on its eastward flank was enhancing outflow from Hope (see Fig. 34 for satellite imagery view). Outflow in this northwest sector does not appear as prominent in the composite (Fig. 32) due to averaging. This region is most often dominated by penetration of inflow due to northeasterlies about the Asian monsoon anticyclone during the summer, or westerlies during the transition seasons (see Fig. 28). These circulation features dominated the majority of slower intensifying cases

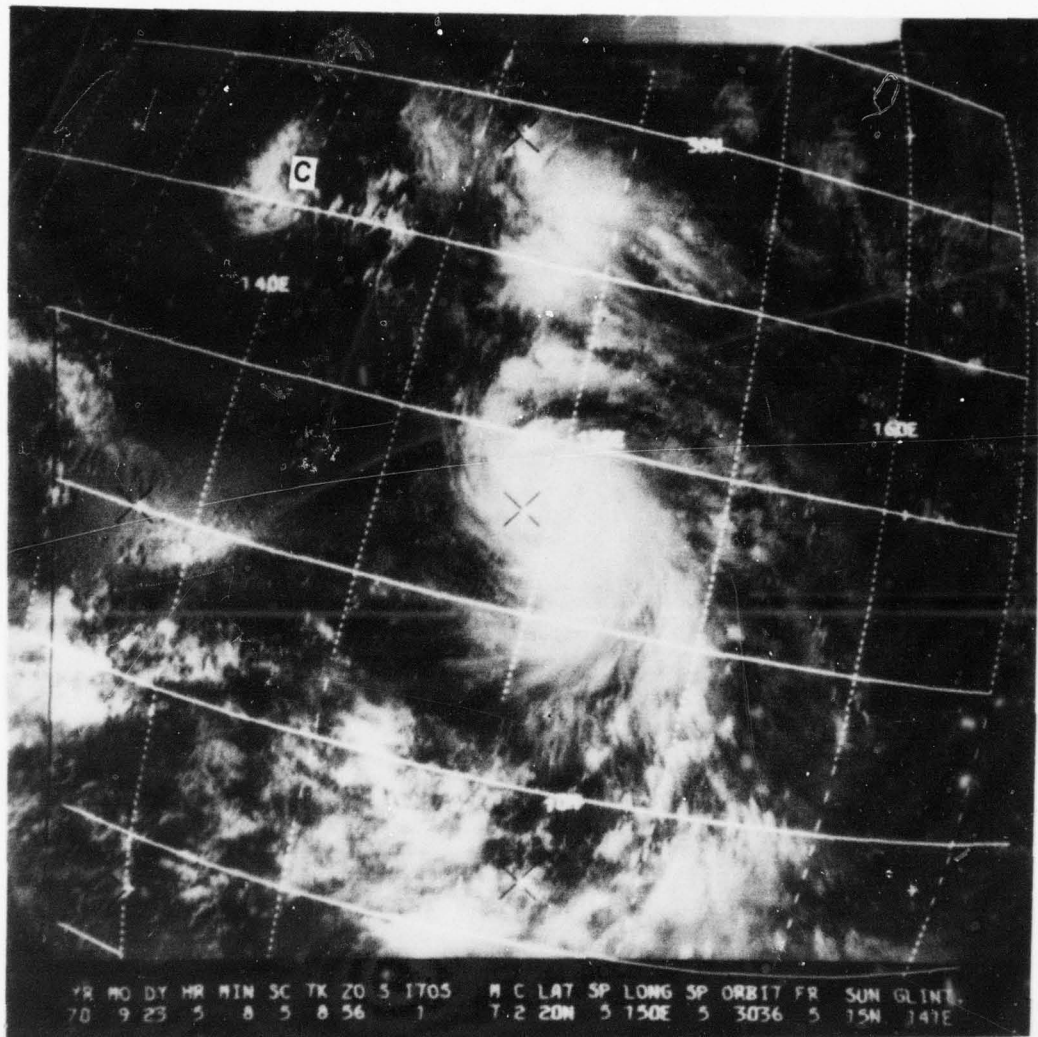


Fig. 34. ITOS-1 satellite view of typhoon Hope (23 September 1970) that depicts typhoon outflow interaction with upper tropospheric cold low 700 n mi to the northwest (c).

in this quadrant. The result is rather apparent in the composite (Fig. 33) as well as Table 7b, with neither the 300° nor 330° sector showing evidence of outflow.

One typhoon in the more slowly intensifying group (Helen 1972) possessed outlets to the north and east as well as the southwest. This suggests that multi-directional outflow as an indicator of the development type also needs to be assessed in terms of its magnitude. Thus radial components for each 30° sector for the 5°, 7½° and 10° radial rings were totaled algebraically for each typhoon to note if differences existed (see Table 8). Radial component net flow's for rapidly deepening storms were found to range between 382 to 456 kt with a mean near 424 kt. In comparison, those cases of less than average deepening varied between 67 and 163 kt with a mean (124 kt) less than one third (29%) of the rapid growth storms. The values of this measure determined from Figs. 32 and 33 were 425 kt and 132 kt, respectively.

An attempt was made to account for the relative size of the typhoons by determining the radius of the 1000-mb isobar from post-analyzed surface charts prepared by the Japan Meteorological Agency. It is noticeable here that the storms displaying a more restrained growth exhibit a slightly larger size in the mean (radius of the 1000-mb isobar of 3.3°, vs. 2.6° for more vigorous development). Since typhoons of various sizes may exhibit differing magnitudes of outflow, the total outflow measure for each typhoon was divided by the radius of the 1000-mb isobar (in degrees latitude) to provide normalized magnitudes for comparison (column 3, Table 8). The variation

Table 8. Total Flow, 5-10° from Center, and Size of Typhoon

Typhoon (Yr)	Total Flow (kt)	a. Extreme Deepening (≥ 60 mb per day)		
		1		3
		Radius 1000 mb isobar [†]	Total Flow/Radius	Radius 1000 mb isobar [†]
Olga (70)	409	1.5	272.7	
Hope (70)	382	2.0	191.0	
Joan (70)	397	2.5	158.9	
Amy (71)	436	1.5	290.7	
Irma (71)	447	2.0	223.5	
Billie (73)	394	1.5	262.7	
Nora (73)	437	2.5	174.8	
Nina (75)	451	3.0	150.3	
Elsie (75)	428	1.5	285.0	
June (75)	456	3.0	152.0	
Mean	423.7	2.1	216.2	
Std. Dev.	±26.3	±.61	±57.5	

Typhoon (Yr)	Total Flow (kt)	b. Slow or Normal Deepening (≤ 24 mb per day)		
		1		3
		Radius 1000 mb isobar [†]	Total Flow/Radius	Radius 1000 mb isobar [†]
Lola (72)	137	3.5	39.1	
Alice (72)	104	2.5	41.6	
Heien (72)	129	2.0	64.5	
Ida (72)	67	2.5	26.8	
Marie (72)	121	4.0	30.2	
Olga (72)	163	3.0	54.3	
Gilda (74)	132	3.5	37.7	
Polly (74)	94	3.5	26.8	
Elaine (74)	130	4.0	32.5	
Irma (74)	168	4.5	37.3	
Mean	124.5	3.3	39.1	
Std. Dev.	±30.4	±.78	±12.0	

[†]degrees of latitude

between extreme deepening typhoons ranged from 150 kt to 285 kt with a mean of 250 kt. The slow to normal developing storms showed less of a range (27 to 65 kt) by contrast, with a mean about 1/6th (16%) of that for more significantly intensifying typhoons.

No typhoon with a 1000-mb isobar radius of less than 1.5 latitude degrees was used in the study. In order to check comparative magnitudes, the radial component analysis for hurricane Celia performed by Clark (1975) was used (see Fig. 35). This hurricane intensified rapidly 200 n mi off the Texas coast on 3 August 1970. A pressure fall of 43 mb in a 15-h period was observed in aircraft reconnaissance observations. The total radial wind component for the 5-10° band about the center summed to 214 kt, and the 1000-mb isobar size measured near 1°. Therefore the result of 214 kt compares favorably¹¹ with the data listed for column 3 in Table 8a. It is interesting to note that the outflow channels for Celia are to the west and south with inflow from the east penetrating close to the center. This is quite uncharacteristic of the rapidly deepening typhoon cases studied, as no outflow is observed toward the east in Celia. Westerlies were well removed to the north but an upper tropospheric low was noted to the southwest, thus enhancing outflow to the west. It also perhaps emphasizes that as long as multi-directional outflow exists with sufficient magnitude, directional preference may be of less importance.

¹¹The outflow level utilizing cloud wind vectors and supplemental rawinsonde data in Clark's study fit better with the 150-mb level.

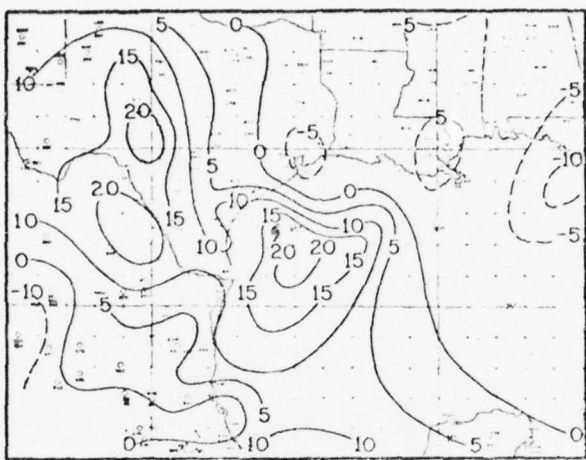


Fig. 35. Radial wind component field (m s^{-1}) for upper tropospheric level (150-mb), Hurricane Celia, 1600 GMT 3 August 1970.

7. SUMMARY

Several characteristics regarding rapid intensification of tropical cyclones in the western North Pacific have been identified in this observational study. These include:

- a) The majority (75%) of the deep central pressures (≤ 920 mb) recorded in the region are attained through the rapid growth process. The bulk (67%) of these pressure reductions occur over a short time span of 18 h or less, although occurrences of ≥ 1.75 mb h^{-1} in the remainder have extended to 36 h. The largest drop observed is most likely to occur during the first 6 h of the period. Relatively few typhoons exhibit a moderate rate of pressure fall preceding this phenomenon; the rapid deepening process is normally abrupt with sharp departures from extrapolation noted (Type 2, 64%).
- b) Rapid deepening is dependent on the organizational state of the storm circulation system. The majority (85% of cases) of onset of rapid development commenced 6 h before to 24 h after typhoon generation. The preceding development period for a weak circulation to strengthen before accelerated intensification requires at least $3\frac{1}{2}$ to 4 days. Onset of this rapid deepening appears more frequently at night than during the day.
- c) The size of the eye encompassed by the cloud wall has some bearing on future development. Most frequently diameters of 20 n mi were observed, and always diameters were ≤ 35 n mi at the onset of rapid deepening. This is in contrast to the

average eye size of 30 n mi. Marked eye size reduction is also noted to be prevalent with vigorous intensification.

- d) Little relation can be found between trajectory direction and speed (or changes of these two variables) and the rapid deepening of a typhoon. There is a tendency for storms traveling faster than normal to decelerate during the deepening process while those initially moving at slow speeds display a gradual acceleration.
- e) Most cases of rapid growth of typhoons occur in the latitude bands 15-20° N during the summer and early fall in an area beginning some 300 n mi east of the Philippines and stretching eastward to the vicinity of the Marianas. During the rest of the year, less frequent activity is observed as the band shifts 5° equatorward. The peak seasonal frequency of significant intensification occurs between 16 September and 15 October. A conspicuous (but unexplained) absence of rapid intensification is observed for the last half of October.
- f) Ocean temperature $\geq 28^{\circ}$ C at a depth of 30 m appears necessary to support rapid development.
- g) Characteristics of the tropical upper tropospheric circulation play the dominant role in determining intensity changes. In particular, the mean position of the Tropical Upper Tropospheric Trough during the summer and early fall and the Subtropical Ridge (November-May) appear to determine the poleward extent of rapid deepening over warm waters ($\geq 28^{\circ}$ C).

- h) The availability of multiple outflow channels from the typhoon to the larger-scale circulation is necessary for rapid growth. Normally this is accomplished by outflow avenues near 200 mb furnished by the Tropical Upper Tropospheric Trough or subtropical westerlies toward the eastern semicircle, and the easterly jet toward the western semicircle. However, variations can exist, often due to the placement of upper tropospheric cold lows relative to the center.
- i) The net radial wind component field at the 200-mb level (5-10° ring from the center) is indicative of rapid growth at the time of onset of rapid deepening. Totals of near 400 to 450 kt appear to be required for most sizes of typhoons (1000-mb isobar at sea level $\geq 1.5^\circ$ in radius). However, smaller size typhoons may exhibit smaller values of the total outflow measure.

8. RECOMMENDATIONS

The following recommendations are made concerning future investigations of tropical cyclone rapid intensification:

Cirrus cloud vectors computed from continuous (30 min) geostationary satellite imagery are needed to fill in the data voids of the tropical western Pacific. Although quite useful, high-level cloudiness features from single-pass, polar-orbiting satellites do not provide quantitative information concerning velocity magnitudes. This requirement may be met after a geostationary satellite (Japanese) becomes positioned over this region in mid-summer 1977.

The sample of cases used in the study could be increased greatly by including the years 1967 through 1969, when operational satellite data first became available. Collecting these data and the needed transient aircraft observations as well as conventional rawinsonde data was impractical for this study due to the time constraints.

Examination of upper tropospheric radial wind component fields should be extended to 24 and 48 h prior to the onset of extreme deepening. Evidence of differences in configuration and magnitude of these fields compared to those 24 h later may show that circulation features leading to rapid deepening are established well in advance of the actual onset. In addition, radial mass flux calculations for these storms also might prove revealing.

Typhoons that intensify more gradually but reach deep pressures (≤ 920 mb) should be investigated. This should establish what outflow interaction with the large scale is necessary to control a

more orderly reduction of central pressure, and distinguish such cases from those for which deep pressures were obtained more abruptly.

Studies focused on rapid intensification of tropical cyclones from depression to typhoon strength in less than a day should be undertaken. Efforts should be directed to obtaining statistics of the event, as well as studying upper tropospheric influences.

REFERENCES

Atkinson, G. D. and C. R. Holliday, 1977: Tropical cyclone minimum sea level pressure/maximum sustained wind relationship for the western North Pacific. Mon. Wea. Rev., 105, 421-427.

Bell, G. J., 1975: Observations on the size of the typhoon eye. Proceedings of World Meteor. Org. Tech. Conf. on Typhoon Modification, World Meteor. Org. Pub., 408, 19-29.

Black, P. G., and R. A. Anthes, 1971: On the asymmetric structure of the tropical cyclone outflow layer. J. Atm. Sci., 28, 1348-1365.

_____, H. V. Senn and C. L. Courtright, 1972: Airborne radar observations of eye configuration changes, bright band distribution and precipitation tilt during the 1969 multiple seeding experiments in hurricane Debbie. Mon. Wea. Rev., 100, 208-217.

Brand, S., 1973: Rapid intensification and low-latitude weakening of tropical cyclones of the western North Pacific. J. Appl. Meteor., 12, 94-103.

_____, and R. F. Gaya, 1971: Intensity changes of tropical storms and typhoons of the western North Pacific Ocean. Navy Wea. Res. Fac., Norfolk, Tech. Paper No. 5-71, 201 pp.

Browner, S. P., W. L. Woodley and C. G. Griffith, 1977: Diurnal oscillation of the area of cloudiness associated with tropical storms. Mon. Wea. Rev., 105 (to be published).

Clark, C. L., 1975: On the Intensification of Hurricane Celia (1970). Mon. Wea. Rev., 103, 131-148.

Colon, J. A., 1963: On the evolution of the wind field during the life cycle of tropical cyclones. Nat. Hurricane Res. Proj. Report No. 65, U. S. Wea. Bureau, 36 pp.

_____, and W. R. Nightingale, 1963: Development of tropical cyclones in relation to circulation patterns at the 200-millibar level. Mon. Wea. Rev., 91, 329-336.

Cressman, G. P., 1952: The development and motion of typhoon "Doris," 1950. Bull. Amer. Meteor. Soc., 32, 326-333.

Crutcher, H. L. and Quayle, R. G., 1974: Mariners worldwide climate guide to tropical storms at sea. NAVAIR 50-1C-61, Asheville, N.C., Naval Weather Service Command, 114 pp.

Dunn, G. D., and B. I. Miller, 1964: Atlantic hurricanes, Louisiana State Univ. Press, 81 pp.

_____, and staff, 1964: The hurricane season of 1963. Mon. Wea. Rev., 92, 128-138.

Dvorak, V. F., 1975: Tropical cyclone intensity analysis and forecasting from satellite imagery. Mon. Wea. Rev., 103, 420-430.

Elsberry, R. E., et al., 1975: Statistical forecasts of 24, 48 and 72 h typhoon and tropical storm intensity changes. J. Appl. Meteor., 14, 445-451.

Fleet Weather Central, 1957-59: Annual Typhoon Reports 1956-58. Fleet Weather Central, Guam M.I.

Frank, W. F., 1976: The structure and energetics of the tropical cyclone. Colo. State Univ. Atm. Sci. paper No. 258, Fort Collins, CO. 180 pp.

Frank, N. L., and C. L. Jordan, 1960: Climatological aspects of the intensity of typhoons. Geophys. Mag., 30, 131-148.

Fung, Y. K., 1970: A statistical analysis of the intensity of typhoons: 1958-1968. Royal Observatory, Hong Kong, Tech. Note, No. 9, 18 pp.

Gentry, R. C., 1969: Project stormfury. Bull. Amer. Meteor. Soc., 50, 404-409.

Gray, W. M., 1975: Tropical cyclone genesis. Colo. State Univ. Atm. Sci. paper No. 234, Fort Collins, CO., 121 pp.

_____, and J. S. Shea, 1973: The hurricane's inner core region. II. Thermal stability and dynamic characteristics. J. Atm. Sci., 30, 1565-1576.

Ito, H., 1963: Aspects of typhoon development. Proceeding of the Inter-Regional Seminar on Tropical Cyclones in Tokyo, Japan Meteor. Agency Tech. Report No. 21, 103-119.

Joint Typhoon Warning Center, 1960-77: Annual Typhoon Reports 1959-76. Fleet Weather Central/Joint Typhoon Warning Center, Guam, M.I.

Jordan, C. L., 1958: Estimation of surface central pressure in tropical cyclones from aircraft observations. Bull. Amer. Meteor. Soc., 39, 345-352.

Jordan, C. L., 1961: Marked changes in the characteristics of the eye of intense typhoons between the deepening and filling stages. J. Meteor., 18, 779-789.

_____, 1963: Tracking of Tropical Cyclones. U. S. Navy Weather Research Facility Report 12-0763-075, 39 pp.

_____, and L. E. Fortner, Jr., 1960: The estimation of surface wind speeds in tropical cyclones. Bull. Amer. Meteor. Soc., 41, 9-13.

_____, and L. E. Fortner, Jr., 1961: Reply to: The estimation of surface winds in tropical cyclones by Bell. Bull. Amer. Meteor. Soc., 42, 383-384.

_____, and N. L. Frank, 1964: On the influence of tropical cyclones on the sea surface temperature field. NSF Grant GP-621, Florida State Univ., Tallahassee, 31 pp.

Kurihara, K., and R. E. Tuleya, 1974: Structure of a tropical cyclone developed in a three-dimensional numerical simulation model. J. Atm. Sci., 31, 893-919.

Leipper, D. F., and D. Volgenau, 1972: Hurricane heat potential of the Gulf of Mexico. J. Phy. Ocean., 2, 218-224.

Meyer, J. W., ed., 1971: Airborne severe storm surveillance. Vol. II, Reports of working panels. Tech. note 1970-43, Lincoln Laboratory, MIT, p. 22.

Meyer, W. D., 1973: Data Acquisition and Processing Program: A meteorological data source. Bull. Amer. Met. Soc. 54, 1251-1254.

Miller, B. I., 1958: On the maximum intensity of hurricanes. J. Meteor., 15, 184-196.

Perlroth, I., 1967: Hurricane behavior as related to oceanographic environmental conditions. Tellus, 19, 258-268.

Ramage, C. S., 1959: Hurricane development. J. Meteor., 16, 227-237.

_____, 1971: Monsoon Meteorology. New York, Academic Press, 296 pp.

_____, 1974: The typhoons of October, 1970 in the South China Sea: Intensification, Decay and Ocean Interaction. J. Meteor., 13, 739-751.

Riehl, H., 1954: Tropical Meteorology. New York, McGraw-Hill, 392 pp.

AD-A049 935

AIR FORCE INST OF TECH WRIGHT-PATTERSON AFB OHIO
ON THE RAPID INTENSIFICATION OF TYPHOONS. (U)

F/0 4/2

AUG 77 C R HOLLIDAY

AFIT-CI-78-27

UNCLASSIFIED

NL

2 OF 2

AD
A049935



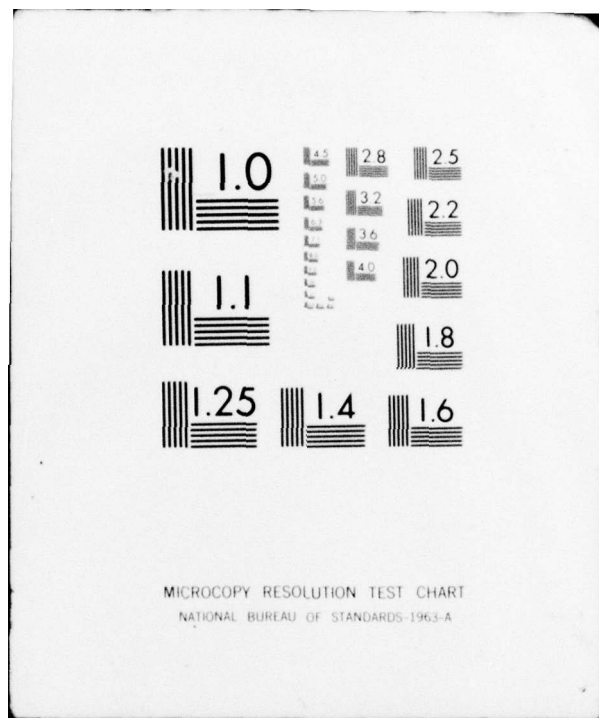
END

DATE

FILMED

3 -78

DDC



Riehl, H., 1956: Intensification of tropical cyclones Atlantic and Pacific areas. U. S. Navy, Bur. of Aero. Project AROWA. Fourth Research Report, Task 12, 28 pp.

_____, 1972: Intensity of recurved typhoons. J. Appl. Meteor., 11, 613-615.

Robinson, M. K., and Bauer, R. A., 1971: Atlas of monthly mean sea surface and subsurface temperature and depth of the top of the thermocline, North Pacific Ocean. Monterey, Fleet Numerical Weather Central, 72 charts.

Sadler, J. C., 1975: The upper tropospheric circulation over the global tropics. Univ. of Hawaii meteor. paper 75-05, 35 pp.

_____, 1976a: Tropical cyclone initiation by the tropical upper tropospheric trough. Mon. Wea. Rev., 104, 1266-1278.

_____, 1976b: Typhoon intensity changes in the Pacific Stormfury area. Univ. of Hawaii meteor. paper 76-02, 50 pp.

Shea, J. S., and W. M. Gray, 1973: The hurricane's inner core region. I. Symmetric and Asymmetric Structure. J. Atm. Sci., 30, 1544-1563.

Sheets, R. C., 1969: Some mean hurricane soundings. J. Appl. Meteor., 8, 134-146.

_____, R. C., 1972: Diurnal Variation in hurricanes NOAA Project Stormfury Annual Report 1971, 121-126.

_____, and P. Grieman, 1975: An evaluation of the accuracy of tropical cyclone intensities and locations determined from satellite pictures. NOAA Tech. Memo., ERL WMPO-20.

Shenk, W. E., and E. B. Rodgers, 1974: Satellite views of hurricane Camille, NASA Tech., Note D-7547.

Sugg, A. L., and J. M. Pelissier, 1968: The hurricane season of 1967. Mon. Wea. Rev., 96, 242-250.

Tannehill, I. R., 1956: Hurricanes. Princeton, Princeton University Press, 308 pp.

Wagoner, R. A., 1973: A technique for using historical analogues to forecast the central pressure of tropical cyclones in the western North Pacific and South China Sea. M. S. Thesis, Texas A&M Univ.

Weickmann, H. K., A. B. Long and L. R. Hoxit, 1977: Some examples of rapidly growing oceanic cumulonimbus clouds. Mon. Wea. Rev., 105, 469-476.

APPENDIX

Typhoons selected for investigation of rapid deepening

Typhoon	Mo.	Year	Max 24 h falli (mb)	Press. at onset (mb)	Type Develop.	Min. Press. (mb)
Sarah	Mar	1956	45	982	2	938
Wanda	Jul	1956	47	979	1	913
Virginia	Jun	1957	73	986	2	884
Agnes	Aug	1957	53	977	2	910
Faye	Sep	1957	47	964	2	933*
Hester	Oct	1957	69	954	1	898
Kit	Nov	1957	42	N/A	2	907
Lola	Nov	1957	58	958	2	896
Doris	Jul	1958	43	975	2	937
Grace	Aug	1958	65	966	2	903
Ida	Sep	1958	88	984	2	877
Nancy	Nov	1958	54	974	2	922
Joan	Aug	1959	61	967	2	891
Vera	Sep	1959	73	964	1	896
Charlotte	Oct	1959	55	975	2	905
Gilda	Dec	1959	46	980	1	914
Harriet	Dec	1959	50	976	2	926
Trix	Aug	1960	50	964	1	935*
Pamela	Sep	1961	62	970	2	906
Violet	Oct	1961	61	960	1	894
Opel	Aug	1962	56	962	1	910
Ruth	Aug	1962	65	981	2	916
Thelma	Aug	1962	50	975	1	946
Emma	Oct	1962	48	965	1	893
Karen	Nov	1962	50	N/A	2	899
Wendy	Jul	1963	49	995	2	925
Carmen	Aug	1963	47	962	1	934*
Bess	Sep	1963	56	N/A	2	930*
Judy	Oct	1963	56	978	2	914
Helen	Jul	1964	46	973	1	931*
Ida	Aug	1964	45	972	1	927
Sally	Sept	1964	65	962	1	896
Wilda	Sept	1964	58	956	N/A	903
Opal	Dec	1964	68	983	2	903

* minimum pressure might have been lower.

APPENDIX (continued)

Typhoon	Mo.	Year	Max 24 h fall (mb)	Press. at onset (mb)	Type Develop.	Min. Press. (mb)
Bess	Sep	1965	58	967	2	905
Carmen	Oct	1965	46	969	1	927
Kit	Jun	1966	79	975	1	886
Cora	Sep	1966	51	990	2	927
Violet	Apr	1967	47	978	2	929
Opal	Sep	1967	69	979	2	910
Carla	Oct	1967	69	979	2	894
Emma	Nov	1967	60	971	1	898
Gilda	Nov	1967	46	958	2	901
Lucy	Jun	1968	57	987	2	935
Wendy	Aug	1968	48	960	1	916
Agnes	Sep	1968	49	951	2	904
Carmen	Sep	1968	48	981	2	922
Elaine	Sep	1968	61	984	2	901
Faye	Oct	1968	43	N/A	1	911
Viola	Jul	1969	46	980	2	891
Ida	Oct	1969	64	995	2	917
Kathy	Nov	1969	43	978	2	929
Olga	Jun	1970	60	978	1	904
Anita	Aug	1970	47	965	2	912
Georgia	Sep	1970	55	959	1	904
Hope	Sep	1970	81	974	1	895
Joan	Oct	1970	65	980	2	901
Patsy	Nov	1970	46	986	2	918
Amy	May	1971	70	975	1	895
Harriet	Jul	1971	45	974	2	929
Lucy	Jul	1971	47	956	1	912
Nadine	Jul	1971	53	960	1	898
Wendy	Sep	1971	48	967	1	915
Bess	Sep	1971	56	962	2	914
Irma	Nov	1971	95	981	2	884
Kit	Jan	1972	54	985	2	933
Billie	Jul	1973	65	986	2	916
Nora	Oct	1973	70	964	2	877
Patsy	Oct	1973	60	950	1	893
Ivy	Jul	1974	44	987	2	945

APPENDIX (continued)

Typhoon	Mo.	Year	Max 24 h fall (mb)	Press. at onset (mb)	Type Develop.	Min. Press. (mb)
Nina	Aug	1975	68	967	1	904
Phyllis	Aug	1975	46	964	1	920
Elsie	Oct	1975	79	983	2	900
June	Nov	1975	89	965	2	876
Olga	May	1976	46	980	2	936
Therese	Jul	1976	68	979	2	905
Billie	Aug	1976	55	960	2	914
Fran	Sept	1976	61	959	1	916
Louise	Nov	1976	52	976	2	895

VITA

Charles R. Holliday was born 31 March 1943 in Missoula, Montana. He is the youngest of two sons of Mabel Peterson, and Terrell C. Holliday. His undergraduate education was received at the University of Maryland with a B.A., in Geography conferred in January 1968. During his undergraduate years he was employed by the U. S. Weather Bureau as a student trainee with assignments in the Washington, D.C. area and Miami, Florida.

Commissioned as an officer in the U. S. Air Force later in 1968, the author attended Texas A&M University in 1969 for undergraduate training in Meteorology under the Air Training Command. He was subsequently assigned to the Joint Typhoon Warning Center, Guam, and served as a forecaster at that unit from 1970-1975. Prior to departing for overseas Captain Holliday married Miss Suzan J. Cameron of Houston, Texas.

The author returned to Texas A&M University in January 1976 to perform graduate study in Meteorology under the auspices of the Air Force Institute of Technology. Captain Holliday is currently assigned to Global Weather Central, Offutt AFB, Nebraska. His permanent address is in care of 5907 Southern Hills Drive, Houston, Texas 77069.

The typist for this thesis was Cindy Brooks

